Spring 2017

Error mapping of build volume in selective laser melting

Ninad Kulkarni

ERROR MAPPING OF BUILD VOLUME IN SELECTIVE LASER MELTING

by

NINAD KULKARNI

A THESIS

Presented to the Faculty of the Graduate School of the

MISSOURI UNIVERSITY OF SCIENCE AND TECHNOLOGY

In Partial Fulfillment of the Requirements for the Degree

MASTER OF SCIENCE

in

MANUFACTURING ENGINEERING

2017

Approved by:

Dr. Frank Liou, Advisor

Dr. K Chandrashekhara

Dr. Heng Pan

ABSTRACT

Selective laser melting is one of the commonly used additive manufacturing processes employed for production of functional part. Therefore, quality aspects such as dimensional accuracy have become a point of great interest. Like all of the other additive manufacturing processes selective laser melting process suffers from the issue if having wide range of process parameters making the process control a complex task. Additionally, issues specific to the selective laser melting process such as position dependency of accuracy of the part, makes it difficult to predict the resulting dimensional inconsistencies in the part manufactured by this processes. This research is an effort to address the issue of part accuracy as a function of part positioning within the build volume. In this research part errors are defined as the function of part location using multiple linear regression model fitting technique. The resulting model is used to develop the understanding of the effect of principle directions onto errors in the part. In addition, a case study has been conducted to validate the model application for different combination of part geometries and part location. The model was found to be useful to accurately compensate part dimensions at same as well as different part locations within the build chamber for parts having same geometry as that of calibration part. The approach can prove to be useful for practical applications such as small batch production reducing part errors thereby requiring lesser post processing work.

Keywords – Selective laser melting, Regression analysis, ANOVA, Part accuracy, Point cloud analysis, Error prediction, Position Dependency of part errors.

ACKNOWLEDGMENTS

I would like to thank my academic advisor Dr. Frank Liou for is constant guidance and support in successfully achieving me graduate degree. I would also like to express my deepest gratitude for his constant guidance to help me develop complex technical expertise that helped me complete my research work. I would also like to thank Dr. K Chandrasekhara and Dr. Heng Pan for providing valuable contribution and recommendations to my research in capacity of thesis committee members.

I would also like to appreciate the assistance and guidance provided by my fellow researcher Sreekar Karnati while conducting the experiments during my research. I would also like the thank Dr. Ming Leu for granting the use of CMM set up.

Finally I would like to express my sincere gratitude towards my parents for their constant blessings and wisdom that help me keep going throughout my research. I would also like to thank all of my friends, for providing encouragement throughout this voyage.

TABLE OF CONTENTS

LIST OF ILLUSTRATIONS

LIST OF TABLES

1. INTRODUCTION

Selective laser melting is one of the powder bed fusion type additive manufacturing processes as per ASTM F42 committee. Since its inception, selective laser melting process is employed in industrial applications across wide spectrum of industries that includes aerospace industry, medical industry, automobile engineering etc. In the recent years, selective laser melting process has matured into manufacturing functional parts from prototype fabrication. Hence, research on attributes such as dimensional accuracy, resulting mechanical properties, surface characteristics etc. have become point great interest. This research is an effort to contribute into dimensional accuracy of the parts manufactured by selective laser melting process.

A typical SLM process begins with a CAD file made by the engineer. The CAD file is then converted into a STL file to input the production instructions such as layer thickness, scanning speed, laser power etc. The STL file is then fed into a SLM machine, which carries out, the production instructions stored in the STL file. The characteristic layer-by-layer production begins with a roller/wiper distributing the layer of powder on the build platform. The powder in the layer is then melted by laser following the path that is nothing but the one of the sectional geometries of the final part. Once the laser scan is complete the wiper places next layer of the powder over while removing additional powder on the powder bed. This way the process repeats itself until the complete part is completely manufactured. After the part is completely manufactured the build platform is raised to the original level and the additional powder is removed and the part is cut from build plate.

Figure 1.1 illustrates the typical SLM process set up from which one can identify major components in the set up. These components majorly include laser source that emits laser beam followed by scanning mirrors also known as Galvano mirrors that deflects laser beam to obtain desired geometry. Laser beam is then passed through plano-convex lens to achieve required spot diameter which one the vital factors in controlling the size of melt pool. Apart from components controlling laser beam parts such as powder scraper i.e. a roller/wiper, build platform etc. plays a vital role in controlling the parameters such as layer thickness, depth of melt pool etc. In this research, attention is focused on the former set of components as they control the factors varying in horizontal direction.
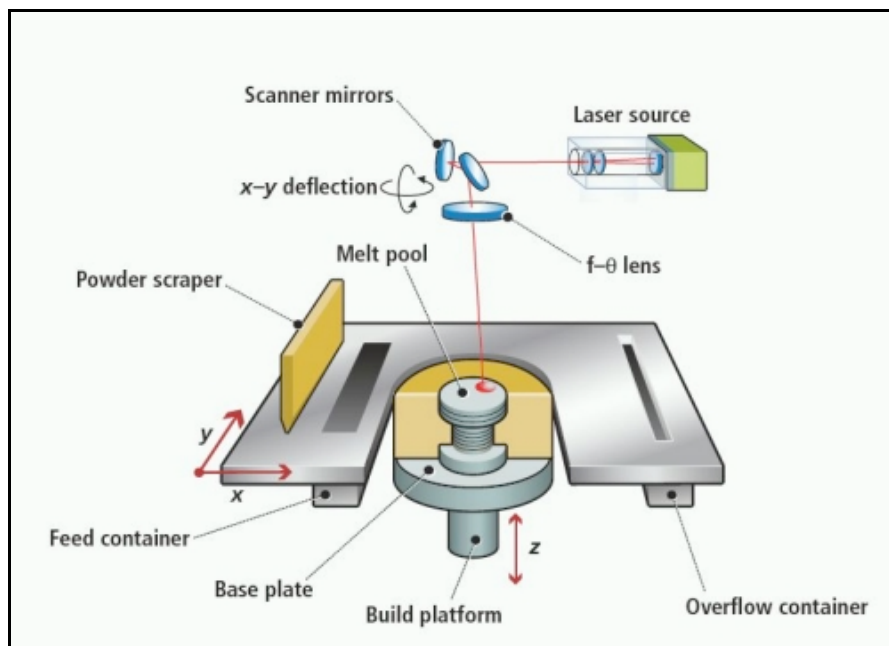
Figure 1.1: Selective Laser Melting Set up

With such a system level description about the SLM process one can figure out that there are number of parameters to be considered while making a part using SLM process. Such a wide variety of parameters make the control of SLM process a highly complex task. Owing to a complex process control of SLM techniques, it becomes difficult to obtain final part within expected tolerance limits of dimensions or mechanical properties. Often to meet the tight tolerance specifications of dimension or mechanical properties parts fabricated using SLM processes are subjected to different post processing techniques. These techniques are specific to what properties are to be altered. For instance, in order to attain better mechanical properties, parts are heat-treated or to achieve desired dimensional specification parts are subjected to machining processes. The machining process involves process such as polishing to improve surface roughness or de-burring process after removing support structures. For the purpose of this research, attention is focused on the dimensional accuracy aspect of the of the SLM process. Even though subtractive post-processing techniques promise to achieve design specifications they would fail in the cases where enough material is not available for removal. In the other words, subtractive post- processing methods are not useful in case of negative material allowance. In order to achieve required machining allowance, it is imperative that adequate offset has to included in the original part design. However, additional offset not only increases the build time but also incurs material wastage in machining of the part. Hence, the machining offset needs to be optimized in order to avoid wastage of material and build time. In order to address this issue current methods pertaining to prediction of dimensional accuracy are reviewed as a part of this research. These methods are broadly classified into two categories as modeling methods and empirical

methods. It was found that most of these techniques are applicable to additive manufacturing processes in general but they do not account for some selective laser melting process specific aspect. The said process specific aspect considered in this research is the position dependency of errors of selective laser melting. Building on this foundation an accuracy prediction method is developed to ensure an only necessary amount of additional material is used to compensate for machining allowance.

Finally, a generic procedure is proposed to ensure optimized non-negative machining allowance for post processing of parts manufactured by selective laser melting process. The procedure is implemented on the commercially available selective laser-melting machine Ranishaw AM250. Details of the experimentation can be found in later sections. The procedure is validated for two different part designs and was found to be in acceptable range. The procedure can be used for either commercial available SLM machines or while accounting for position dependent errors in Hybrid manufacturing centers.

2. LITERATURE REVIEW

The purpose of this research is to evaluate effect of position of part within the build chamber on the accuracy of the part. Hence, an exhaustive literature survey has been conducted to determine current state of the art of the existing methods researched to predict or evaluate accuracy of the selectively laser melted parts. From the literature review it was found that to address issues pertaining to dimensional accuracy in SLM process, there are broadly two approaches followed by engineers and researchers as mentioned bellow:

- Process modeling approach.
- Process qualification approach.

Both of these approaches are discussed in this section with their merits and demerits. Upon careful evaluation process qualification approach has been followed for the purpose of this research. Finally, an area for improvement is identified within the process qualification approach that serves as a motivation for this research.

2.1. PROCESS MODELING APPROACH

Through extensive research it has been found out that control of resulting mechanical properties as well as the dimensional qualities depend greatly upon size of melt pool (Gockel, Joy et al 2013). This is one the most important reasons why thermal modeling of melt pool is vital for modeling the any additive manufacturing process. Naturally, within the research conducted thus for on modeling the selective laser melting process is driven by making thermal model of the melt pool. A finite element approach is used to evaluate thermal behavior of the melt pool in selective laser melting process

(Zeng, Kai, et al 2012). A typical thermal model would focus on the heat transfer across the melt pool boundary. Generally, laser beam is the heat input where as the heat dissipation occurs via conduction to adjacent solid part or powder particles as well as convection to surrounding medium. With the help of such thermal models researchers have been successful in predicting the residual stress in resulting parts (Zaeh, M. F. et al, 2010, Klingbeil, N. W., et al, 2002, Roberts, 2012). The residual stresses are then attributed to dimensional defects within the parts such as distortions, form errors etc. Another group of researchers have used the finite element approach to predict the anisotropic shrinkage in SLM process (Paul, R., 2013, Wang, 2007). The anisotropic shrinkage is then transformed into dimensional errors inside the manufactured parts. Generic models for applying such anisotropic shrinkage analysis to compensate for dimensional errors in additively manufactured parts have been provided (Huang, Qiang, et al 2015).

Using modeling approach for evaluating the dimensional accuracy of the parts fabricated by selective laser melting process has a biggest advantage of reducing experimental work. These models can be validated relatively easily as they narrow down range of process parameters. Moreover, depending upon availability of computational power more accurate results can be achieved.

However, in all of the research conducted following modeling approach it is assumed that the boundary conditions would remain the same through out the build chamber of selective laser melting set up. However, in reality considerable difference can be noted within the environmental conditions of build chamber. For instance, depending up one location of gas flow nozzle different velocities of inert gas can be observed at

different locations (Dadbakhsh, S.,2012, Ferrar, B., et al., 2012). Another example of different boundary conditions can be change in the size of spot diameter owing to random scattering of laser beam. Accounting such variability while modeling the selective laser melting process can prove to be computationally challenging. Additionally, inclusion of variable conditions as a function of part location would be at the cost of a few assumptions such as laminar flow of inert gas, which may widen the margin of error. Another possible source of error for process modeling approach is the loss of accuracy owing to conversion of CAD file to STL file format. Transitioning from CAD file, which is essentially a B-rep data file to a STL file compromises accuracy of original design. These errors have to be accounted for while accepting results of validation experiments. Hence, it was decided not to pursue the modeling approach for to address the research problem at hand.

2.2. PROCESS QUALIFICATION APPROACH

The process qualification approach relies extensively on experimental analysis of the selective laser melting process. This approach is widely used in the realm of predicting capability of a particular additive manufacturing set up to produce various features such as thin walls, narrow holes, overhangs etc. For implementation of this philosophy, first a standard part is designed consisting all the desired features required to determine the set up capability. Such standard part is then printed using the set up under consideration. The parts are then measured and examined against the original design to compute the errors. Once the set up is calibrated in this way, it can be used to expedite the process planning for selective laser melting techniques. Although, this approach

requires extensive experimentation as compared to process modeling approach, it circumvents making assumptions about the variable environmental conditions within the built chamber. Hence, this approach considered useful for the purpose of this research. Several efforts have been taken to design parts for qualifying the particular process or a machine set up. For example, a standard part illustrated in Figure 2.1(Kurth et al, 2005) was designed to investigate various features such as circular features (hole, fillets), thin walls, over hangs, sharp corners etc. This part was also used to determine other entities such as surface roughness as well as mechanical properties etc.
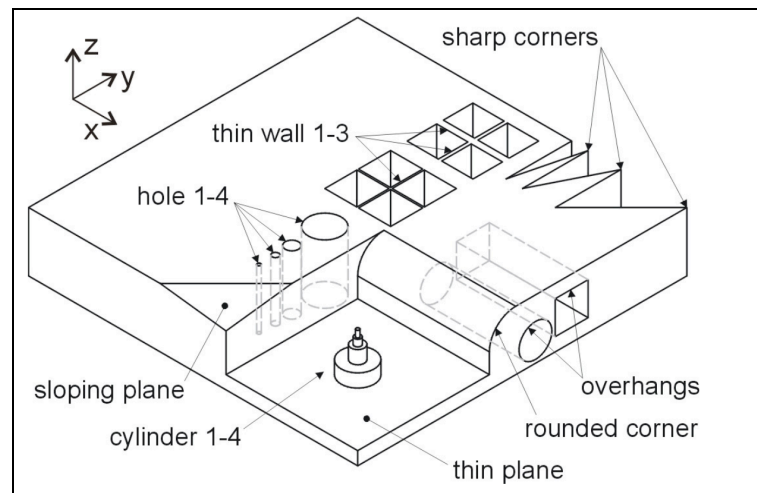
Figure 2.1: Calibration Part designed by Kurth et al

Another example implementing similar concept but more focused on to evaluate capability of build set up to create features at various angles is illustrated in Figure 2.2 (Castillo, Laura 2005). One of the recent standard calibration parts which provided basis for evaluation of thirteen different errors is illustrated in Figure 2.3 (Moylan, Shawn, et

al. 2012).   Although these parts provide excellent means to evaluate capability of a

particular set up to create particular feature, these parts do not account for evaluation of

part accuracy on the basis of the location of a particular part.
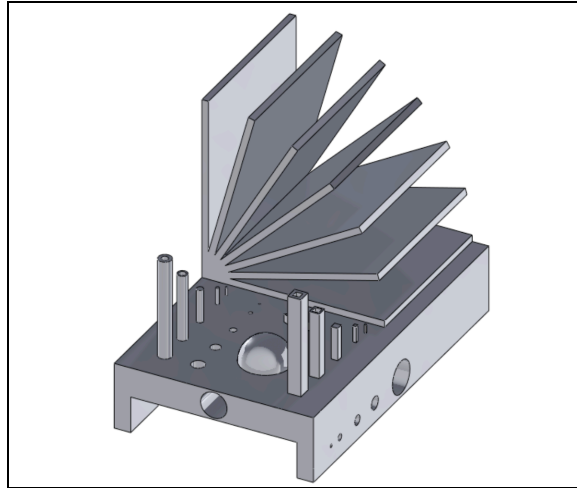
Figure 2.2: Calibration part by L. Castillo
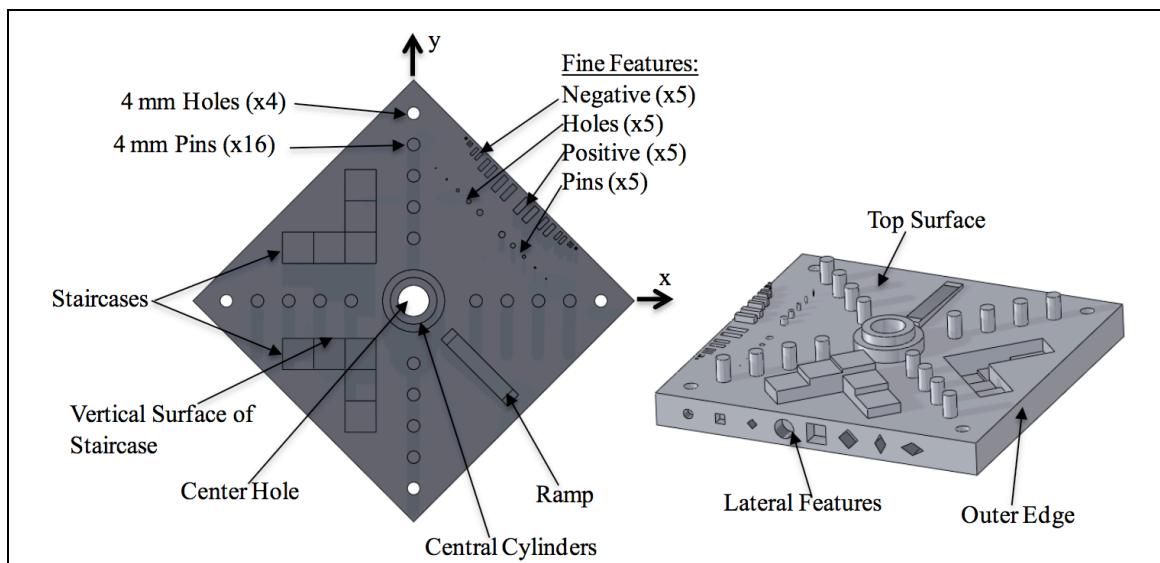
Figure 2.3: Calibration Part by Moylan

Unlike the aforementioned standard part designs there one can find examples of some calibration parts, which can be seen as more aligned to goal of this research. Figure 2.4 (Kleszczynski, S., et al., 2015) shows a test part used to measure the effect of part location within the build chamber to surface roughness of the part. In this work surface roughness of all of the nine parts has been measured. It was found that the value of surface roughness increases as the part is moved radially outward from the center of the build chamber. However, the purpose of this study was to understand trend in the change of surface roughness value based on the position of the part as well as the angle of the part to the x-y plane, this part may not be considered as ideal design to be pursued for current research problem.
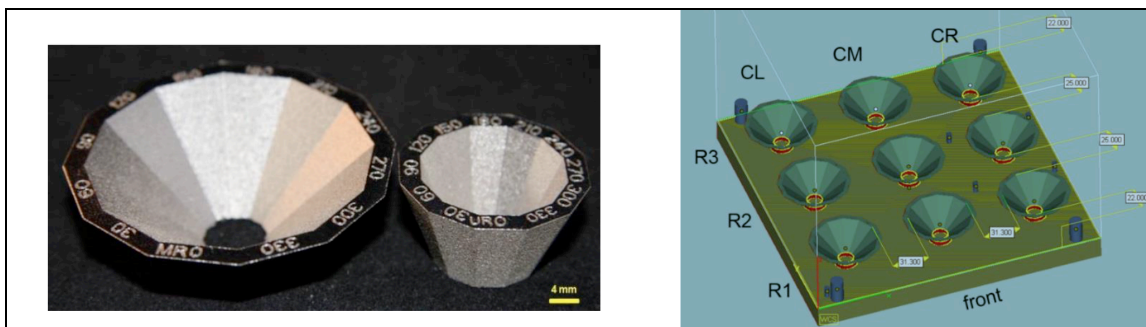
Figure 2.4: Test part set up by Kleszczynski, S., et al.

Figure 2.5 (Brøtan, Vegard, 2014) illustrates a standard part comprising a 5x5 array of 20 mm diameter cylinders. In this case, radius of each cylinder is estimated by taking multiple points along the circumference of each cylinder followed by applying least square method to minimize the radius of each cylinder. The grid location of each cylinder is acts as an optimization constraint for evaluation of radius of cylinder. The

measurement is carried out using a pre-calibrated CMM touch probe. In this research,

deviation in the part dimension as a function of the location of part is clearly established.

However, it is to be noted that the part accuracy is mapped only in the X-Y directions

where as a separate staircase like structure was built to assess the set up accuracy in the

Z- direction. In the other words, influence of Z direction on the part deviation in X-Y

plane cannot be understood using this method. Similarly relation between part deviation

in Z direction and location of part within the build chamber is not discussed in the current

work. These considerations are addressed while deigning a part for current research
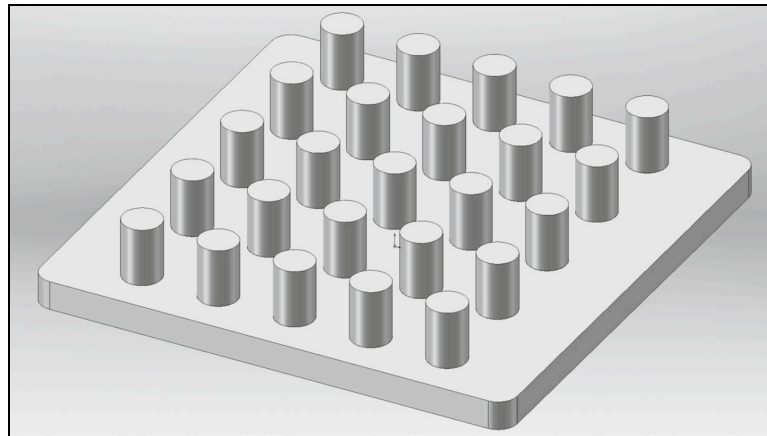
problem.

Figure 2.5: Calibration part by Brøtan, Vegard

3. METHODOLOGY

As already mentioned in previous section it has been decided to follow process qualification approach to address the current research problem. In this section, the entire process of evaluating the research problem is discussed. At first objectives for process qualifications were established. After setting the objectives individual task such as design of calibration part, setting up experimental conditions, analysis of results, measurement strategy has been carried out in order to fulfill all the objectives. Each subsequent subsection focuses on rationale behind every task, implementation plan and expected results. Such systematic approach proved to be helpful not only to cover all possible situations that may arise post experimentation but also reduced number of experimental trails required.

3.1. OBJECTIVES OF PROCESS QUALIFICATION

Process qualification study is conducted to determine capability of any particular additive manufacturing set up to build a set of certain geometric features. In case of current research problem it has been decided to study the effect of location of a part within the build chamber on the dimensional errors of the part. Hence, entire experimental analysis was focused on following objectives:

1. Selection of set up for fabrication of parts and process conditions.

2. To determine the variation of error in part dimensions in X-Y plane with respect to Z direction.

3. To determine the variation of error in part dimensions in Z direction as function of part position within the build chamber.

4. Prepare the measurement strategy for taking the measurements of predefined

    features in the part and a method of obtaining the part errors.

The above-mentioned objectives form a basis to define the entire experimental

strategy. These objectives either individually or collectively helped narrowing down the

focus onto each sub task in the development of entire qualification process. The sub

tasks are discussed in following sections.

3.2.   SELECTION OF TEST SET UP

Test set up is the additive manufacturing equipment that will be used to

manufacture the part. For this research, additive manufacturing equipment in

consideration is Ranishaw AM-250 machine at Missouri S&T, Rolla. Selecting the said

set up imparts additional constraints to the process design because the entire study is now

bound by the limits of operating parameters of the Ranishaw AM-250 machine. Fixing

the manufacturing equipment helps defining the dimension of build volume. The

dimension of build volume is one of the driving factors in deciding the dimensions of the

calibration part. In case of Ranishaw AM-250 machine the maximum dimension of the

build volume is 250mm wide, 250mm wide and 300mm tall. This research focuses

majorly on the variation of part error along build chamber only the smaller section of the

build chamber is selected instead of the entire build chamber. Reducing the size of build

chamber has allowed for considerable savings in material and production time while

obtaining cogent proof of concept. The dimensions of build volume utilized for the

current study are as shown in Figure 3.1.
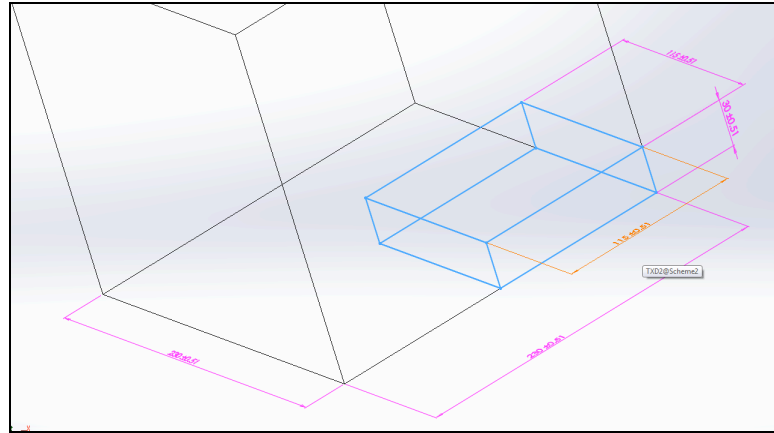
Figure 3.1: Build volume section for process

Because this study does not take in account for variation of most of the operating parameters in its current state, no further investigation is conducted along this dimension. Hence, all the processing conditions such as laser power, scan speed layer thickness etc. are maintained at the same value for each build. This way it is ensured that errors obtained in the part would be exclusive of the process conditions.

3.3.   DESIGN OF CALIBRATION PART

The design of calibration part is driven by first two objectives of the process. In order to achieve first objective it is imperative that multiple measurements have to be taken at different values of Z co-ordinates keeping the same value of X-Y coordinates of the same feature or part. This could have been achieved by using a simple cuboid geometry at different locations within the build chamber. However, if this part geometry is followed the second process objective cannot be achieved which requires the features in the part with ability to measure errors along Z direction at different combination of absolute coordinate locations of the part. One way to address this issue is to have two

separate parts to comply with each objective. Such examples can be found in development of calibration parts (Iuliano et al, 1994). However, having two different parts will not only increase the number of experiments required but also add a source of error when the two models are combined together. Hence, it was decided follow a stair case geometry in a pyramid like structure as shown in Figure 3.2. Using this geometry the distance between opposite step rises can be useful for calculating the dimension error along any of the horizontal directions. On the other hand height of each step can be measured to obtain the error in Z direction.

Another consideration to account for while designing a calibration part is to define the datum for position of the part. This datum position will play an important role in relating the errors to a particular location. For each measured feature datum reference was decided as the centroid of the feature. While deciding the centroid of the feature as a datum reference an assumption is made that the dimensional error will be uniform along the centroid of the feature. To verify this whether condition is satisfied, the centroid of each feature was computed and mapped onto relative location of the ideal design. As no significant error was observed in the location of the centroids for each feature the centroid of the feature was assigned as a location of that particular feature. Sample analysis of the measurement can be found later sections.

Once the overall geometry of the part was finalized the dimensions of the part have been determined. One of the major constraints while deciding part dimensions was the size of build volume. In order to analyze dimensional errors on account of part placement it was imperative that exactly same features have to be placed at different

location within the build chamber. Hence, a grid consisting nine parts was made as shown in Figure 3.3. The detailed layout drawing can be found in Appendix A.
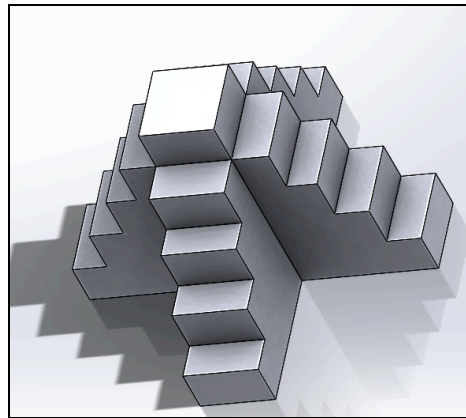
Figure 3.2: Preliminary part geometry

Once the overall geometry of the part was finalized the dimensions of the part have been determined. One of the major constraints while deciding part dimensions was the size of build volume. In order to analyze dimensional errors on account of part placement it was imperative that exactly same features have to be placed at different location within the build chamber. Hence, a grid consisting nine parts was made as shown in Figure 3.3. The detailed layout drawing can be found in Appendix A.

In this way the final calibration part set up provides three distinct measurement levels in each X and Y-axis as well as five distinct level of measurement along Z direction for analyzing errors in horizontal plane. In addition it provides eighteen distinct measurements along each X and Y direction for four different levels of Z direction measurements for determining errors along Z direction.
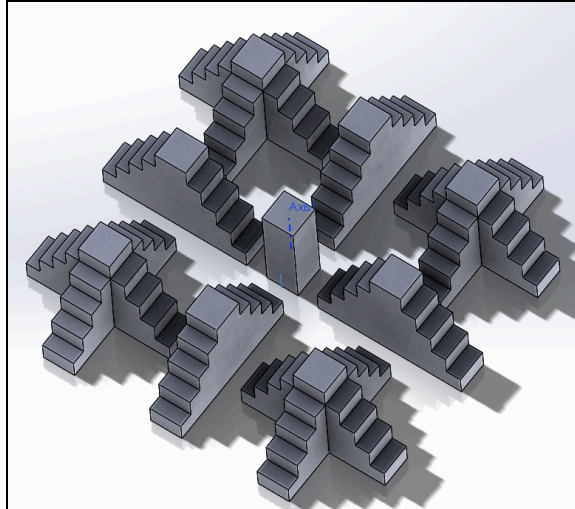
Figure 3.3: Final part design

3.4.   MEASUREMENT STRATEGY

Selection of measurement set up is the central part of measurement strategy. For measuring the dimensions of various features different alternatives of measurement equipment were available. These set ups include caliper device, coordinate measurement machine (CMM), a custom apparatus using a laser sensor mounted on a CNC machining center and 3D laser scanner. One of the major criteria for narrowing down onto one measuring devices was the measurement accuracy. For the purpose of this study accuracy it was decided that measurement accuracy should be better than 0.05mm. Hence, 3D scanner set up with accuracy of 0.2mm was not considered for the measurement.

Out of the remaining three alternatives laser sensor set up was rejected because of its inability to access inter features of the calibration part grid. The laser sensor could not access the inner feature of the part due to it was too big to move between the space available between the parts on the grid. Finally out of the two remaining alternatives CMM set up with a touch probe has be selected for measuring the printed part owing to

satisfactory accuracy requirement of 0.02mm and ability to access all the sections of the part. The CMM machine superseded the calipers as the calipers could not provide means to compute the centroid of the feature being measured. As mentioned in Section 3.3 estimation of centroid is one of the key derived requirements of part design.

The CMM setup used for this study was Brown & Sharp Reflex 343 with Ranishaw touch probe (TP-ES). Figure 3.4 shows one of the test parts under measurement.
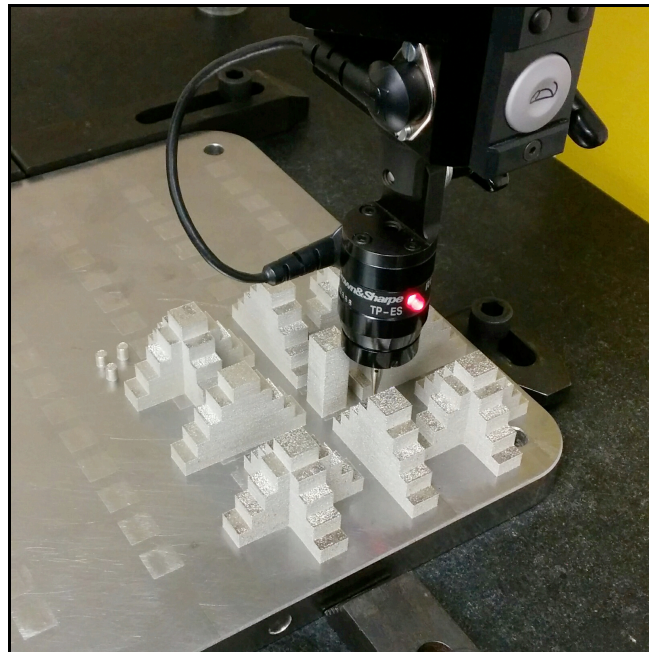
Figure 3.4: Part measurement on CMM

Using CMM set up coordinates of different points was measured. There were two type of features used for picking up the points. One of the features is the rise of the step and another one is the floor of the step. Both these features were planner and differed

only in one of the dimensions which as height. The rise had the height of 6mm where as the floor was 4.5mm wide. Giving total area of 60mm^2 and 45mm^2 respectively. For locating rise of the step 60 points were taken in the grid of 15 X 4 where as for the floor 36 points were measured in the gird of 12 X 3 (Frank David, 2001). Such measurement strategy lead to a point cloud of 10080 point-measurements per part. In addition, different points on the substrate plate were measured to which were used as a horizontal plane for aligning the point cloud with the CAD model.

After the point-measurements were completed in order to compute the required feature dimensions post processing of point-cloud data was carried out using MATLAB 2014Ra software. The point cloud data was first filtered to remove error measurements such as points noted accidentally while moving the probe etc. The MATLAB code for this exercise can be found in Appendix B. The data filter code also provided sorting the measurement data in XY, YZ and XZ planes.

The sorted data point cloud data was aligned with the actual CAD model by fitting planes on each feature individual as well as collectively (Li, Xudong, et al. 2013). Method of minimizing the least squares was used for fitting the plane on to each and feature (Eberly, David, 2000). In addition to fitting a plane to each individual step rise a plane is fitted to set of three step rises having at least two same location co-ordinates along X and Y axis. These planes were examined for perpendicularity with each other as well as with the plane fitting to point cloud data taken from the substrate plate. Once it was confirmed that the all these planes were mutually perpendicular the equation of the intersecting line for the outermost planes along X & Y axes was computed (Weisstein, Eric W. 2002). The point of intersection of this line with the plane fitted to substrate plate

was the found, which was nothing but origin for the actual build volume. Using this point

the homogenous transformation matrix for translation was computed and used to transfer

the point cloud from CMM co-ordinate reference frame to ideal co-ordinate reference

frame. Finally the angle between the YZ plane and plane fitted to outer most features of

along –Y axis direction was computed. This angle was used to compute homogenous

transformation matrix for rotation along Z axis to align the point cloud data with actual

CAD file. Figure 3.5 shows the aligned ideal and measured point clouds.
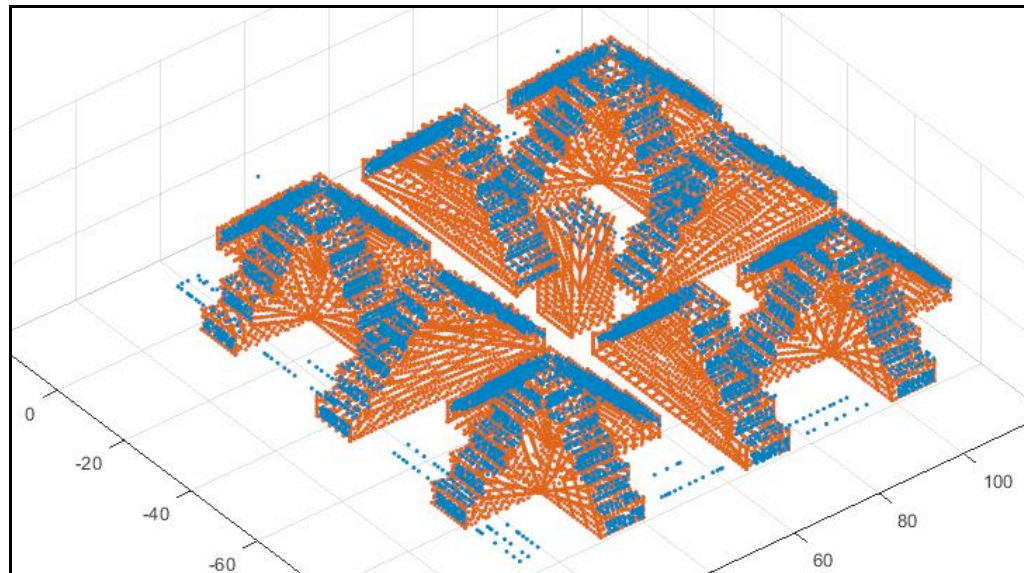
Figure 3.5: Aligned point clouds

For computation of feature dimension, distance between the two fitted planes on

the opposite side of one feature is calculated. It is worth noting that the distance

considered here is the global distance between planes and not the point-to-point distance.

Once the distance between two planes is calculated location of the centroid of the each

feature is calculated for each part of on the grid. It was observed that all the centroids

belonging to each feature for a given part are collinear and the line joining all the

centroids is parallel to Z-axis proving the errors are symmetrically distributed along the

centroid of the feature.

3.5.   STATISTICAL MODELING

3.5.1. Multiple Linear Regression Model. In order to determine the effect of
each co-ordinate a statistical approach is followed. It was decided that a multiple linear

regression model would be fitted to estimate the effect of each direction as a multiple

linear regression model can express the error as a function of each co-ordinate along a

particular dimension. A general form of multiple linear regression model with single

response variable y, and k predictor variables or regressor xj is given by equation (1).

$$y = \beta_0 + \sum_{j=1}^{k} \beta_j x_j + \epsilon \tag{1}$$

From equation (1) it we can identify two terms namely β and ϵ. The term β are

sometimes known as the regression coefficients where as ϵ is the model error. The

regression coefficients provide influence of a particular regressor onto the response

variable. In the other words, equation (1) can be used to describe a hyper plane in k-

dimensional space of regressor variable x_j. This way one can capitalize on the parameter

β_j to estimate the change in response variable y for given change in a corresponding

regressor variable x_j while all other independent regressor variables are kept constant. As

far as model error (ϵ) is concerned plays an important role in estimating the regression

constant.

For applying the multiple linear regression model to present research problem it is necessary to define the regressor and response variables in the model. As the effect of co-ordinate locations on the dimensional error in given direction is to be studied, error in the given direction is considered as response variable. Naturally, the three co-ordinate locations of features were assigned to the three predictor variables. As discussed in Section 3.4, errors were calculated independently in all the three directions. Hence, three distinct multiple linear regression models were generated for dimensional error along each direction. This way the generalized form of multiple linear regression model can be reduced for present case as given by equation (2-4).

$$X\_Error = \beta_{0x} + \beta_{1x}X + \beta_{2x}Y + \beta_{3x}Z + \epsilon \tag{2}$$

$$Y\_Error = \beta_{0y} + \beta_{1y}X + \beta_{2y}Y + \beta_{3y}Z + \epsilon \tag{3}$$

$$Z\_Error = \beta_{0z} + \beta_{1z}X + \beta_{2z}Y + \beta_{3z}Z + \epsilon \tag{4}$$

It is obvious from equations (2-4) that there are three regressor variables for one response variable with four regression coefficients and model error. The model won't be useful unless the values of regression coefficients are estimated. For estimation of regression coefficients method of least squares (Montgomery, Douglas C, 2008) is used. In this method, the least square function given by square of the model errors is minimized with respect to regression coefficients. The corresponding values of regression coefficients those minimize the least square function are known as least square estimators. For calculation of least square estimators Minitab 17 software package was used. It should be noted that for using least square method to calculate the least square estimators, the number of observations of each response variable should be greater than number of regressor. Now one build of the calibration part provides one set of

observations for error in all three directions. This suggests that there are at least four builds required for calculating least square estimators. Once, the least square estimators are calculated, these values are substituted in the original multiple linear regression model. Such modified model is termed as fitted regression model. The fitted regression model is useful in predicting influence of regressor onto response variables. In addition fitted model can be used to estimate the values of response variables for entire range of regressor variables. Thus using multiple linear regression model method provides a tool to satisfy both objectives of the research problem. The actual models for errors in all the three directions can be found in Section 4.

3.5.2. ANOVA Analysis. It should be noted that while using multiple linear regression models it was assumed that all the three variables would influence the response variable independently. Hence, the combined effect of two or all three parameters is not considered while fitting a regression model. However, in practice there is a possibility that two or all the three regressor can have a notable effect on the error in that particular direction. Statistically this phenomenon is termed as interaction between the regressor variables. In order to, support the assumption that there is no interaction between the regressor variables ANOVA analysis for carried out on the data before the model fitting is carried out. In ANOVA analysis corrected sum of squares is used for all individual and interacting regressor variable combinations. This technique provides statistically justified means to assess the regressor variable interaction by computing p value for given significance level. In the current analysis significance level of 0.05 is used. The ANOVA analysis was conducted using SAS software package. Details of ANOVA analysis are mentioned in Section 4.

4. RESULTS AND ANALYSIS

4.1. ERROR MEASUREMENTS

After each run of experiment, the part measurements have been taken using CMM set up. The CMM point cloud data is aligned with ideal CAD file using MATLAB 2014Ra.The measurement methodology and error calculation procedure has been discussed in Section 3.3. In this section the measurement data for build number 4 has been discussed. The measurement data for other three builds can be found in the Appendix C. Figure 4.1 illustrates an example of aligned point cloud for build number 4.
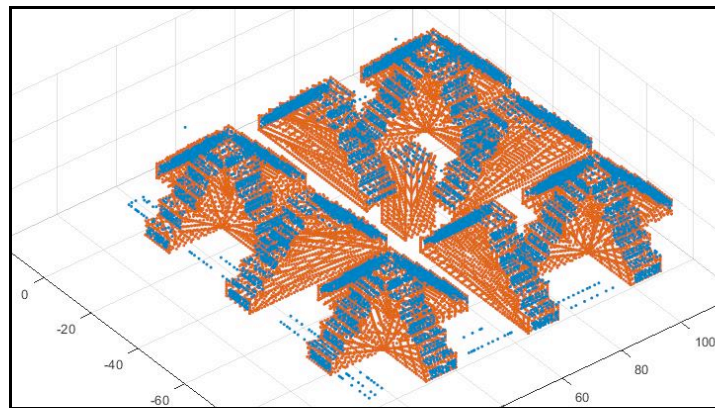
Figure 4.1: Point Cloud Alignment

As discussed in Section 3.5 it is required to estimate the errors in each direction separately and has to be modeled as a function of the part location. This is achieved by formatting the data as shown in Table 4.1. The Table 4.1 summarizes the data giving two levels of X locations, three levels of Y locations, and five levels of Z locations with total combination of 30 observations. In order to study the trend in variation of error in the X direction with respect to any other direction one can keep the other two directions at

constant levels varying the third dimensions. For example, if effect of change of Z

coordinate of the feature is on the error is X direction is to be studied then, X and Y

location of the feature can be maintained at fixed level say X at 92 and Y at 23. This will

refer to the last column and first five rows after the header row of the Table 4.1. Here it is

evident that the error in X direction is increasing with the increase in Z co-ordinate.

Similar trends can be found for all other combinations of co-ordinates. However,

analyzing error variation for each build separately can be a tedious and time-consuming

effort. Hence, a linear model is fitted to the data obtained by all four builds following

multiple linear regression method as explained in Section 3.5.1. Table 4.2 tabulates error

measurements in Y direction.

Table 4.1: Error measurements in X direction

Y Co-ordinate	Z Co-ordinate	Ref. Dim.	X =23			X =92		
			Measured Value	Error	% Error	Measured Value	Error	% Error
-23	3	46	46.260	0.260	0.56	46.144	0.144	0.31
	9	37	37.211	0.211	0.57	37.116	0.116	0.31
	15	28	28.194	0.194	0.69	28.100	0.100	0.36
	21	19	19.168	0.168	0.89	19.153	0.153	0.81
	27	10	10.145	0.145	1.45	10.173	0.173	1.73
-57.5	3	46	46.327	0.327	0.61	46.259	0.259	0.56
	9	37	37.257	0.257	0.69	37.226	0.226	0.61
	15	28	28.262	0.262	0.94	28.172	0.172	0.61
	21	19	19.242	0.242	1.27	19.112	0.112	0.59
	27	10	10.206	0.206	2.06	10.229	0.229	2.29

Table 4.1: Error measurements in X direction (cont.)

Y Co-ordinat	Z Co-ordinat	Ref Dim.	X = 23			X=92		
			Measured Value	Error	% Error	Measured Value	Error	% Error
-92	3	46	46.290	0.290	0.63	46.198	0.198	0.43
	9	37	37.228	0.228	0.62	37.102	0.102	0.28
	15	28	28.213	0.213	0.76	28.166	0.166	0.59
	21	19	19.173	0.173	0.91	19.168	0.168	0.88
	27	10	10.161	0.161	1.61	10.184	0.184	1.84

(All dimensions in mm)

Table 4.2: Error measurements in Y direction

X Co-ordinate	Z Co-ordinate	Ref. Dim.	Y =-23			Y =-92		
			Measured Value	Error	% Error	Measured Value	Error	% Error
23	3	46	46.2403	0.240	0.52	46.3273	0.327	0.71
	9	37	37.1720	0.172	0.46	37.2116	0.212	0.57
	15	28	28.1414	0.141	0.50	28.2486	0.249	0.89
	21	19	19.1331	0.133	0.70	19.2180	0.218	1.15
	27	10	10.1085	0.108	1.08	10.1871	0.187	1.87
57.5	3	46	46.2809	0.281	0.61	46.3350	0.335	0.73
	9	37	37.2013	0.201	0.54	37.2601	0.260	0.70
	15	28	28.1448	0.145	0.52	28.2706	0.271	0.97
	21	19	19.1833	0.183	0.96	19.3029	0.303	1.59
	27	10	10.1830	0.183	1.83	10.2871	0.287	2.87
92	3	46	46.2369	0.237	0.51	46.1734	0.173	0.38
	9	37	37.1957	0.196	0.53	37.2778	0.278	0.75
	15	28	28.1856	0.186	0.66	28.1839	0.184	0.66
	21	19	19.1607	0.161	0.85	19.2455	0.245	1.29
	27	10	10.1784	0.178	1.78	10.1999	0.200	2.00

(All dimensions in mm)

Error measurement in Z direction is taken with respect to a fixed reference. The base plate is considered as a fixed datum in this particular case. Additionally, as one of the prime objectives of this study is to measure the variation of error in Z direction with respect to part location multiple Z measurements are taken at 4 levels of Z co-ordinates, and nineteen levels of X and Y co-ordinate locations each.

4.2. ANOVA FOR REGRESSOR INTERACTION

In order to apply regression analysis of with distinct predictor variables it is required to check for interaction between the regressor variables. As it is decided to use the multiple linear regression model, the interaction between two first order regressor variables at a time is to be evaluated. In addition, the interaction among all the regressor variables is also of great interest so as to decide whether said interaction term is to be used or not. SAS software package is used to carry out ANOVA analysis on the regressor variables. Details of ANOVA analysis on for each response variable i.e. the error in the given direction and the corresponding regressor variables i.e. the location co-ordinates are discussed in the following subsections (4.2.1 -4.2.3).

4.2.1. ANOVA For Error In X Direction. For performing ANOVA on X direction errors the data from all four runs was compiled and randomized before inputting into SAS software package. Using GLM procedure with interactive mode and default confidence interval of 95% the ANOVA was performed. The sample source code for the program can be found in Appendix D. The part of output i.e. is the ANOVA table is represented by Table 4.3. From the table it is evident that all the regressor variables have

significant effect on the variance in response variable, as the p value for the regressor

variables is less than 0.0001. Additionally, for source of variability due to interaction

terms X*Y, Y*Z and X*Y*Z, p value is higher than 0.05. Higher p value implies that the

interaction terms have no significant effect and can be ignored from the model. However,

for the interaction term X*Z the p value is lesser than the accepted value of 0.05. This

implies that the interaction of X*Z has a significant effect on the response variable and

the term should be added to the multiple linear regression model. However, adding

another term calls for additional build creation. Additional build would add to increased

number of experimental trials, which would include additional cost and time. Hence, for

the purpose of current research the interaction term is ignored from the general multiple

linear regression model.

Table 4.3: ANOVA table for Errors in X direction

Source	DF	Type III SS	Mean Square	F Value	Pr > F
X	1	0.07494791	0.07494791	84.07	<.0001
Y	2	0.14667403	0.07333702	82.26	<.0001
X*Y	2	0.00071832	0.00035916	0.40	0.6696
Z	4	0.03864502	0.00966125	10.84	<.0001
X*Z	4	0.02647394	0.00661849	7.42	<.0001
Y*Z	8	0.00845827	0.00105728	1.19	0.3164
X*Y*Z	8	0.01314577	0.00164322	1.84	0.0792

4.2.2. ANOVA For Error In Y Direction. ANOVA on errors in X direction
for performing ANOVA on Y direction errors, the data from all four runs was compiled
randomly and fed into SAS software package. Using GLM procedure with interactive
mode and default confidence interval of 95% the ANOVA was performed. The part of
output i.e. is the ANOVA table is represented by Table 4.4. Like the errors in X direction
for the errors in Y direction all the regressor variables have a significant effect on
response variable owing to p value under 0.05. On the other hand interaction terms X*Y,
X*Z and X*Y*Z are insignificant as the p value is higher than 0.05. Therefore these
terms can be dropped from the model. For the interaction term Y*Z the p value is lesser
than the accepted value of 0.05 making the interaction term significant in the multiple
linear regression model. However, just like the case of X*Z interaction for errors in X
direction, it was decided to ignore Y*Z interaction term from the general multiple linear
regression model.

Table 4.4: ANOVA table for Errors in Y direction

Source	DF	Type III SS	Mean Square	F Value	Pr > F
X	2	0.04570572	0.02285286	9.21	0.0002
Y	1	0.31389896	0.31389896	126.47	<.0001
X*Y	2	0.01275086	0.00637543	2.57	0.0822
Z	4	0.05239581	0.01309895	5.28	0.0007
X*Z	8	0.01707066	0.00213383	0.86	0.5534
Y*Z	4	0.02807744	0.00701936	2.83	0.0292
X*Y*Z	8	0.01114364	0.00139295	0.56	0.8069

4.2.3.   ANOVA For Error In Z Direction. For conducting ANOVA on errors in Z direction exactly same procedure is followed as for the performing ANOVA on errors in X direction or Y direction. The SAS source code-implementing GLM procedure in interaction mode can be found in Appendix D. Table 4.5 gives the ANOVA table from the program output. It can be seen from table 4.5 regressor variables have a significant effect owing to lower p values. On the other hand interaction X*Y interaction has been proven to be insignificant. However for rest of the terms i.e. X*Z, Y*Z, and X*Y*Z the sum of squares is found to be zero. This is because the missing data points in the data model. The case of missing data had arisen because there are total 1296 combinations of possible observations for the given dataset. However, only 98 values were measured in each experiment. Incidentally, over 90% data points are unavailable for the ANOVA. Although it is possible to obtain these values, it will require adding additional features to the calibration part, which may impose measurement limitations in X & Y directions. Hence, the effect of these interactions was considered to be inconclusive and it was decided to move forward with only the regressor variables for fitting the multiple linear regression model. In addition these considerations were proved to be acceptable when other analysis were performed to understand quality of the design model. These analyses includes analysis of residuals where in normal distribution of residuals provides an indication of good fit the equation. Another example of the analysis is analysis of regression constant. Both of these details are discussed in this research in order to establish applicability of the model.

Table 4.5: ANOVA for Errors in Z direction

Source	DF	Anova SS	Mean Square	F Value	Pr > F
X	18	0.10391403	0.00577300	5.76	<.0001
Y	17	0.10465646	0.00615626	6.14	<.0001
X*Y	57	0.06379693	0.00111924	1.12	0.2780
Z	3	0.07016975	0.02338992	23.33	<.0001
X*Z	6	0.00000000	0.00000000	0.00	1.0000
Y*Z	7	0.00000000	0.00000000	0.00	1.0000
X*Y*Z	-13	0.00000000	0.00000000	0.00	.

4.3.   MULTIPLE LINEAER REGRESSION MODEL FITTING

Fitting a multiple linear regression model if the final step in the analysis of the experimental results. Fitting a multiple linear regression model provides means not only to analyze the effect of each direction on the position of the part but also it enables to predict errors for give feature location. The procedure of model application is as discussed in Section 3.5.1. The said procedure is implemented in Minitab 17 software package to obtain the required model for error prediction in each direction. The details of resulting models are discussed in subsequent subsections. The residual plots for all the models are attached in Appendix D

4.3.1. Model Fitting For Error In X Direction. Equation 5 is the fitted model for error in X direction. As already mentioned the X, Y and Z are the co-ordinates of the centroid of each feature measured in millimeters. Also the X_error is the percentage error in the dimension and not the actual error. The percentage error is used so that model can

be used in general application rather than specific geometry. It should be noted that the

regression model as mentioned in equation 5 excludes the effect of interaction of X and Z

co-ordinate locations.

X_error = 0.2424 - 0.000724 X - 0.000547 Y - 0.002077 Z   (5)

The model analysis part from Minitab output is shown in Figure 4.2. The model

analysis confirms the results obtained from ANOVA analysis. Near zero p values signify

that the error in X direction is a function of part location along all the co-ordinates.

```
Model Summary

        S    R-sq  R-sq(adj)  R-sq(pred)
0.0462971  66.13%     64.48%      62.14%


Coefficients

Term            Coef   SE Coef   T-Value   P-Value   VIF
Constant      0.2424    0.0141     17.24     0.000
X          -0.000724  0.000123     -5.91     0.000  1.00
Y          -0.000547  0.000150     -3.64     0.000  1.00
Z          -0.002077  0.000498     -4.17     0.000  1.00
```

Figure 4.2: Minitab 17 Output for fitting model to errors in X direction

4.3.2. Model Fitting For Error In Y Direction. In the similar way as that of

model fitting for X_error, model for errors along Y direction is fitted using Minitab 17.

The fitted model is given by equation 6, in which X, Y and Z are the co-ordinates of the

centroid of each feature measured in millimeters. Also the Y_error is the percentage error

in the dimension and not the actual error. The percentage error is used so that model can be used in general application rather than specific geometry.

$$Y\_error = 0.1761 + 0.000266\ X - 0.001482\ Y - 0.002392\ Z \qquad (6)$$

The model analysis part from Minitab output is shown in Figure 4.3. The fitted linear model proves that location of part in all the directions has a significant influence over the part error. This observation proves the results of ANOVA analysis. It should be noted that the regression model as mentioned in equation 6 excludes the effect of interaction of Y and Z co-ordinate locations.

```
Model Summary

         S    R-sq  R-sq(adj)  R-sq(pred)
0.0536870   72.54%    71.31%      69.01%

Coefficients

Term            Coef    SE Coef   T-Value   P-Value   VIF
Constant      0.1761    0.0163     10.80     0.001
X            0.000266  0.000174     1.53     0.029    1.00
Y           -0.001482  0.000142   -10.44     0.009    1.00
Z           -0.002392  0.000578    -4.14     0.004    1.00
```

Figure 4.3: Minitab 17 Output for fitting model to errors in Y direction

4.3.3. Model Fitting For Error In Z Direction. A multiple linear regression model is fitted for errors in Z direction using Minitab17 in the exactly same way as that of errors in X or Y direction. The fitted model is given by equation 7, relates percentage errors in Z direction to X, Y and Z are the co-ordinates of the centroid of each feature

measured in millimeters. The percentage error is used so that model can be used in general application rather than specific geometry.

$$Z\_error = 0.10735 - 0.000032\ X + 0.000107\ Y - 0.001340\ Z \qquad (7)$$

The model analysis part from Minitab output is shown in Figure 4.4. From the analysis of model coefficients it is observed that the regressor variables X and Y are insignificant where as regressor variable Z and the constant have significant effect on the error in Z direction. Unlike the case of model error in X direction or Y direction the fitted model contradicts the interpretation of ANOVA table for error in Z direction. One of the potential causes for this discrepancy could be the missing data point. However, when the plot of residuals was examined for the same response variable it proved applicability of the model.

```
Model Summary

        S    R-sq  R-sq(adj)  R-sq(pred)
0.0378193  66.48%     65.74%      64.40%


Coefficients

Term           Coef   SE Coef  T-Value  P-Value   VIF
Constant    0.10735   0.00597    17.97    0.000
X         -0.000032  0.000058    -0.55    0.585  1.01
Y          0.000107  0.000057     1.88    0.061  1.00
Z         -0.001340  0.000289    -4.64    0.000  1.01
```

Figure 4.4: Minitab 17 Output for fitting model to errors in Z direction

5. CASE STUDY: MODEL APPLICATION

In Section 4, three distinct multiple linear regression models have been generated. With exhaustive analysis the quality of models have been evaluated. In this section, the model has been applied to reduce the dimensional errors for same part design and different part geometry to study the effect of geometry changes onto the effectiveness of error prediction models. The case study was designed to test a certain objectives as explained in Section 5.1 along with the results in Section 5.2

5.1. CASE STUDY: DESIGN OBJECTIVE & PROCEDURE

Main objective of the case study is to evaluate the usability of error prediction models. Following three cases were planned to determine effectiveness of error prediction models as given by equations (5-7).

- Application of error model to compensate errors in the part of same geometry located at same location as that of calibration part.
- Application of error model to compensate errors in the part having same geometry as that of calibration part but located at different locations.
- Testing the applicability of error model to a part with different geometry than calibration part.

To test above-mentioned objectives a new build was planned on the same set up i.e. Ranishaw AM250 with exactly the same processing conditions as that of previous four runs. Maintaining consistency in process setup and processing condition eliminates errors imparted by these conditions.

There are three sample parts used in the case study as shown in Figure 5.1. The parts A & B have the same geometry as that of parts in calibration runs. In addition, dimensions of part A and B are varied to minimize the error using the error models. Part A is located at the same position as that of calibration run. This way first objective of the study can be tested. Another copy of part A is placed at different location as that of calibration. Part B is also placed at a location other than its original location in calibration run. In this manner part b along with copy of part A placed in different locations are supposed to test the second objective of the study. Part C, however is of entirely different geometry to account for third objective of the case study. Figure 5.2 illustrates the final part layout on the build plate. It should be noted that part 1 and part 3 are the same as part A but at different locations so do the part 4 and part 5 are same as part C. However, error compensation was applied only in part 5 but not part4. Also part 2 is same as part B.
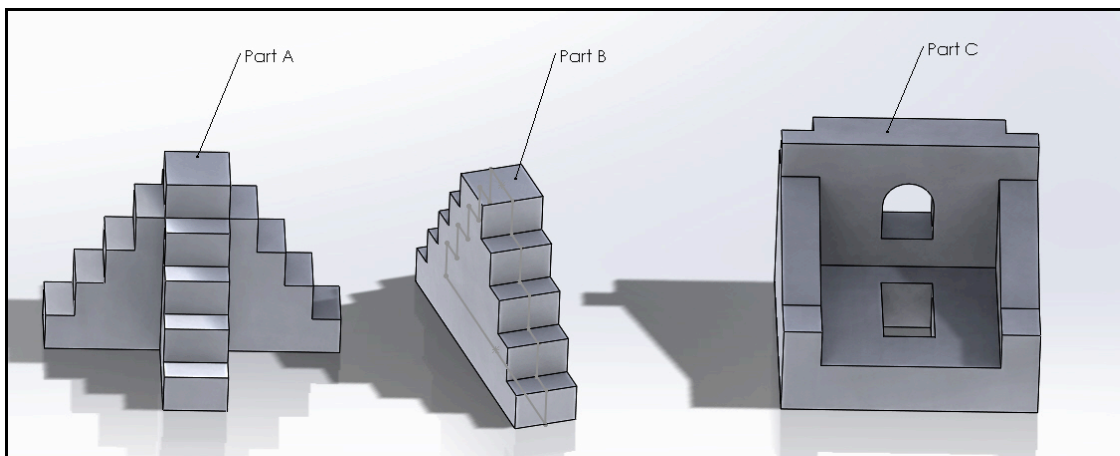
Figure 5.1: Parts used in Case study

After the build is completed part measurements were taken using the same CMM set up that was used for measuring the calibration part. The point cloud data obtained from CMM was then processed using MATLAB 2014Ra software package. Post processing involved a crucial task of point cloud alignment using plane-fitting technique (Li, Xudong, et al. 2013) same as that of point cloud alignment for calibration part. Once the point clouds were aligned part dimensions were calculated. The values of each part dimension are discussed in Section 5.2.
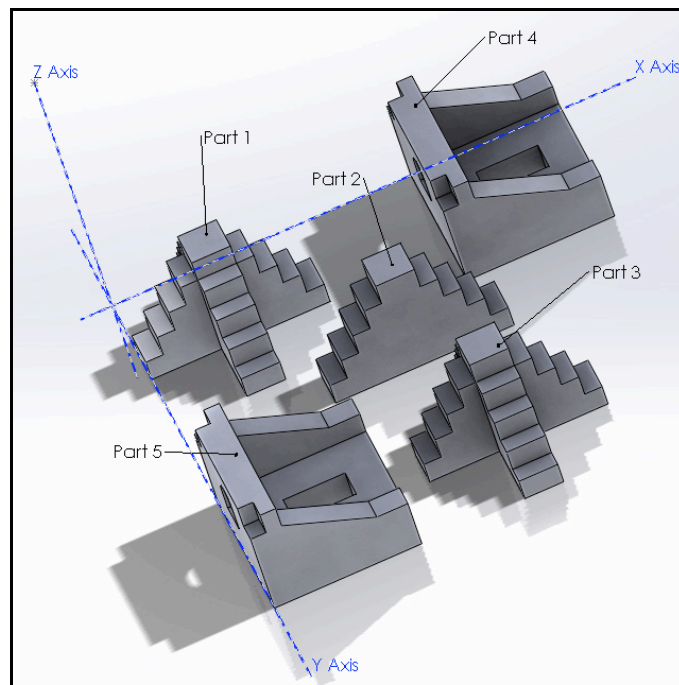
Figure 5.2: Final part layout

5.2. CASE STUDY: RESULTS

In this section the measured dimension are compared with the design specification of all five parts in the final build. The measurement values can be found in Appendix F.

For part 1 the basis of comparison was the dimensions of similar part in one of the calibration build. However, for the rest of the parts the measured error was compared with the residual range for the fitted model. If the error value falls between the range of first residual the model can be considered to have successfully estimated the compensation value. Figure 5.3 shows the dimension measured in each variant of part A. Since geometry of part A is same as part 1 and part 3 similar measurement scheme is used for both the parts.
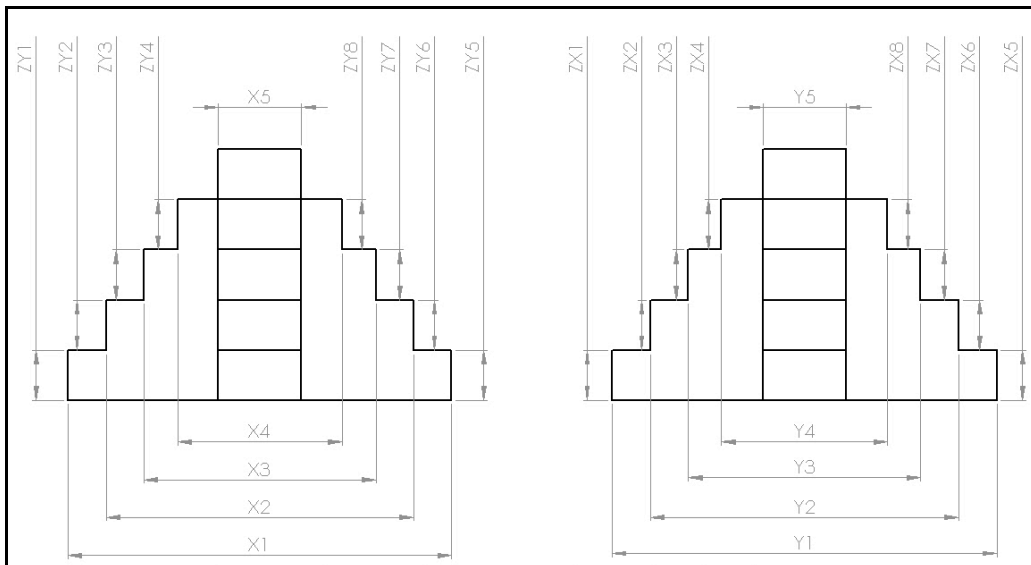
Figure 5.3: Measurement Scheme for Part A

The measured error values for part 1 and error values one of the similar part in build# 3 are compared by plotting the corresponding values of errors. Figure 5.4 illustrates the plot of error measurements of given feature in part 1 against the error measurement of the corresponding feature in similar part in Build#3 for all the three measurement directions. It can be concluded from the plots in Figure 5.4 error after

compensation is less than dimensional errors in a part without any compensation. This proves the first objective of the case study i.e. the error model can be used to minimize error in the part having the same geometry at the same location.
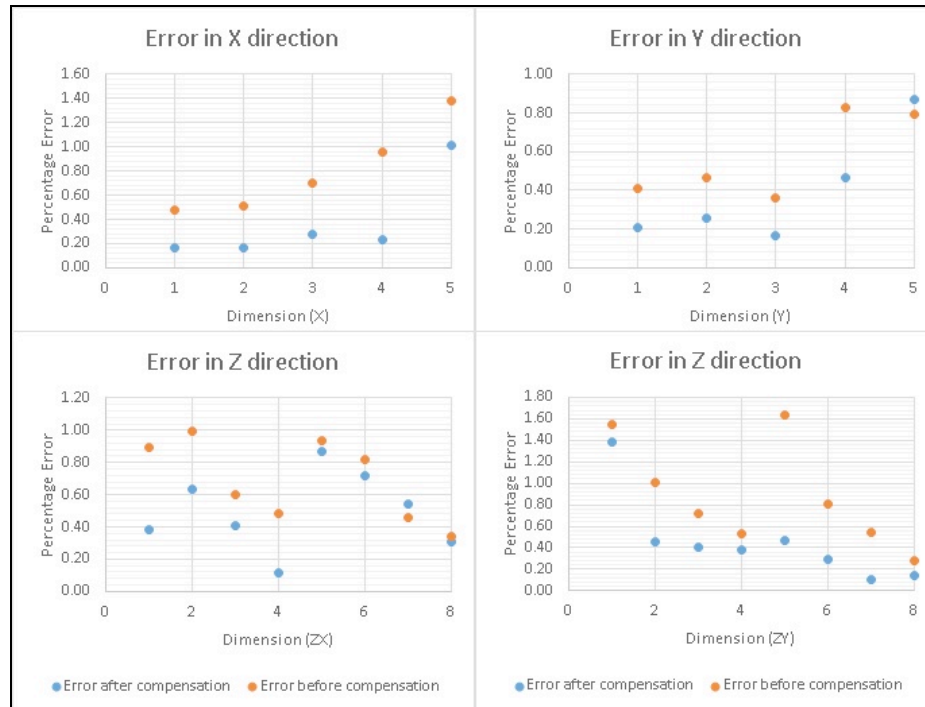
Figure 5.4: Error Comparison Plots for Part 1

Figure 5.5 and Figure 5.6 shows the measurement strategies for parts 2, 4 and 5. From the Figure 5.5 it can be construed that total 5 features were considered while taking measurements in X direction whereas total 8 features were measured along Z direction in part 2. While in part 4 and part 5 four features in each direction were measured as illustrated in Figure 5.6.

As mentioned earlier in this section to test if model can successfully apply compensation in same geometry parts at different location or the part having entirely different geometry the error values were compared with the residual limits for each

model. If all the error value falls within the range of residual limits of a given model it is concluded that the compensation model is successful in applying compensation for a given part. Otherwise it was assumed that the model fails to apply compensation for the said part.
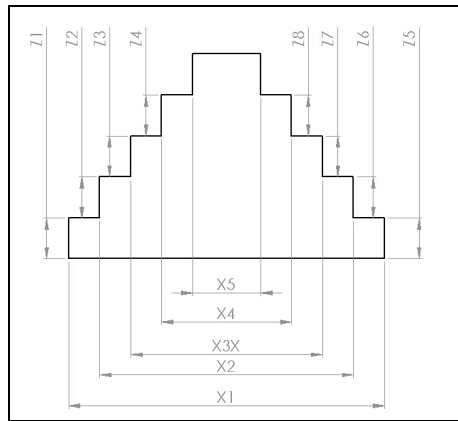
Figure 5.5: Measurement Strategy for Part 2
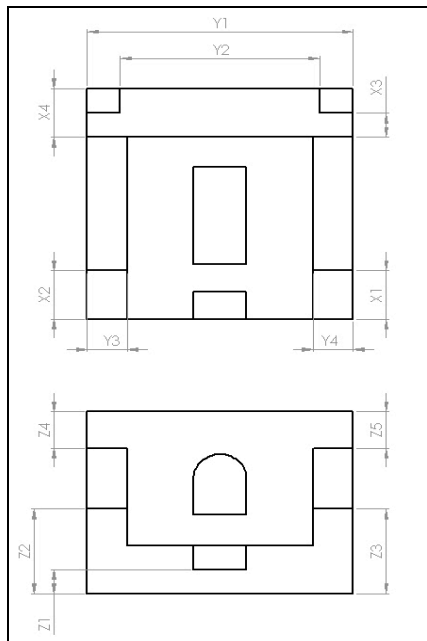
Figure 5.6: Measurement Strategy for Part 4 and 5

The comparison is represented by plotting the error values for given feature against the residual limits. Figure 5.7 and Figure 5.8 shows the residual plots for part error measurements in part 2 and part 3 respectively. In both the Figure it is well established that all the error values lie within the limit of residuals. Hence, it can be said that the model can compensate the errors in parts of same geometry as that of calibration part at different location within the build chamber.
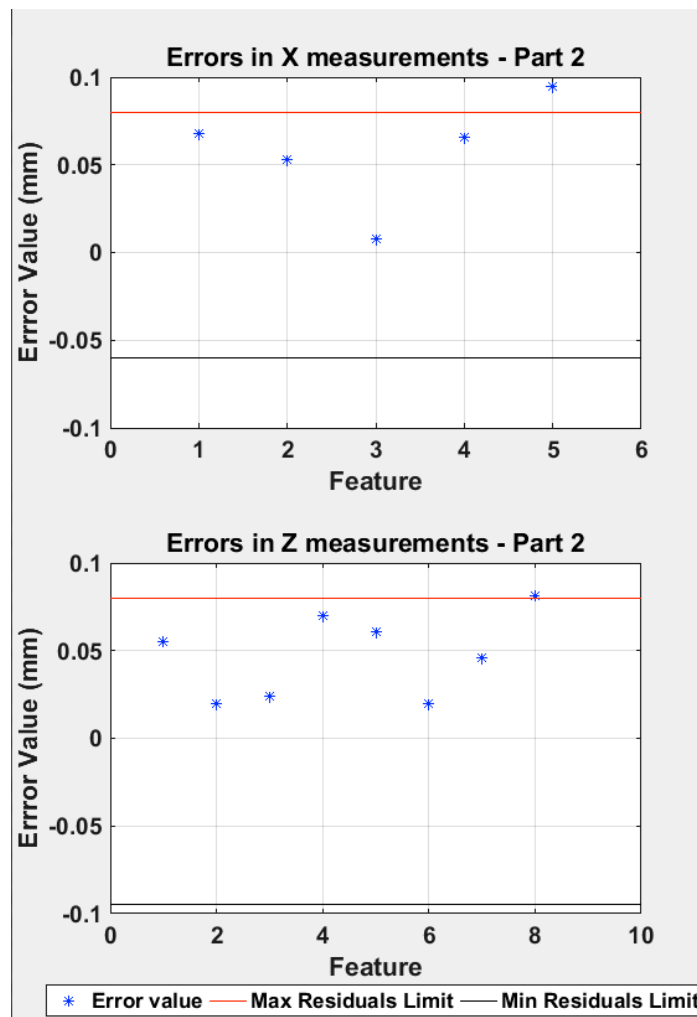
Figure 5.7: Error evaluation for Part 2
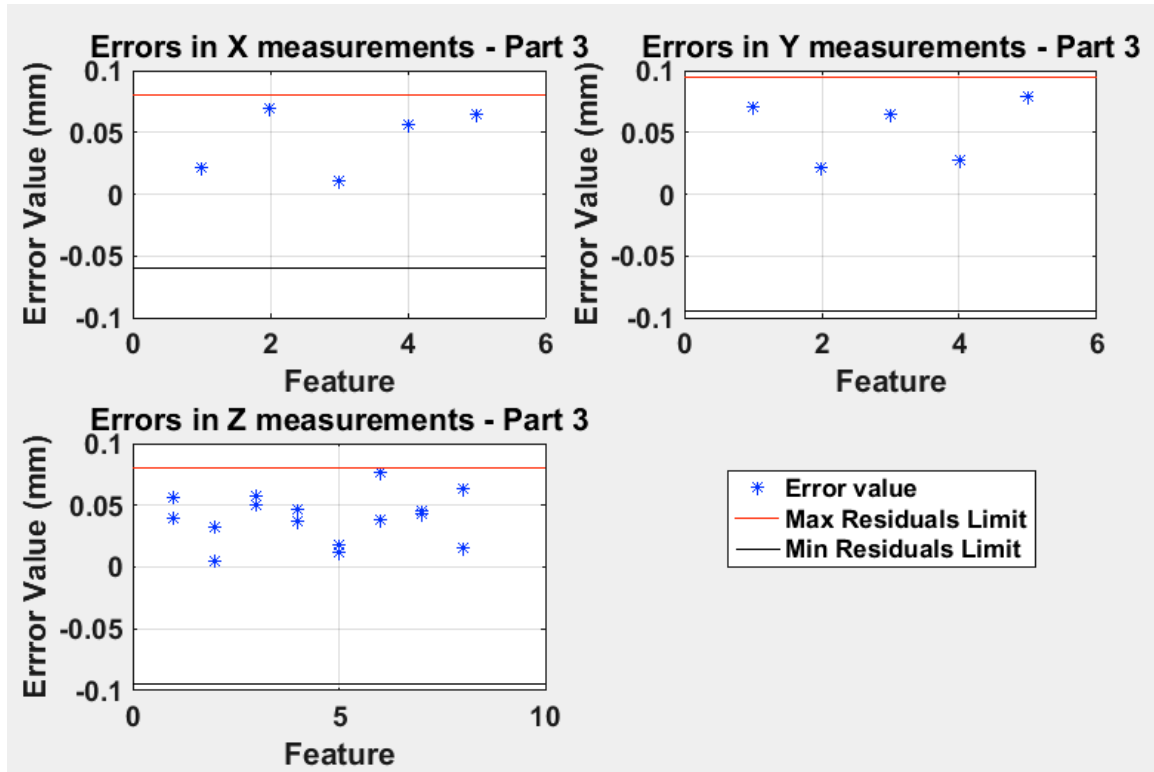
Figure 5.8: Error Evaluation for Part 3

Lastly similar analysis was conducted for part 5 in which the last objective of the study is to be tasted. The comparison of residues for the case of part 5 has been shown in Figure 5.9. From the Figure 5.9 it is evident that the error compensation has not been successfully applied in the part as most of the error values remain outside the residual limit. Hence, it can be understood that model cannot be comprehensively applied to the part having different geometry.
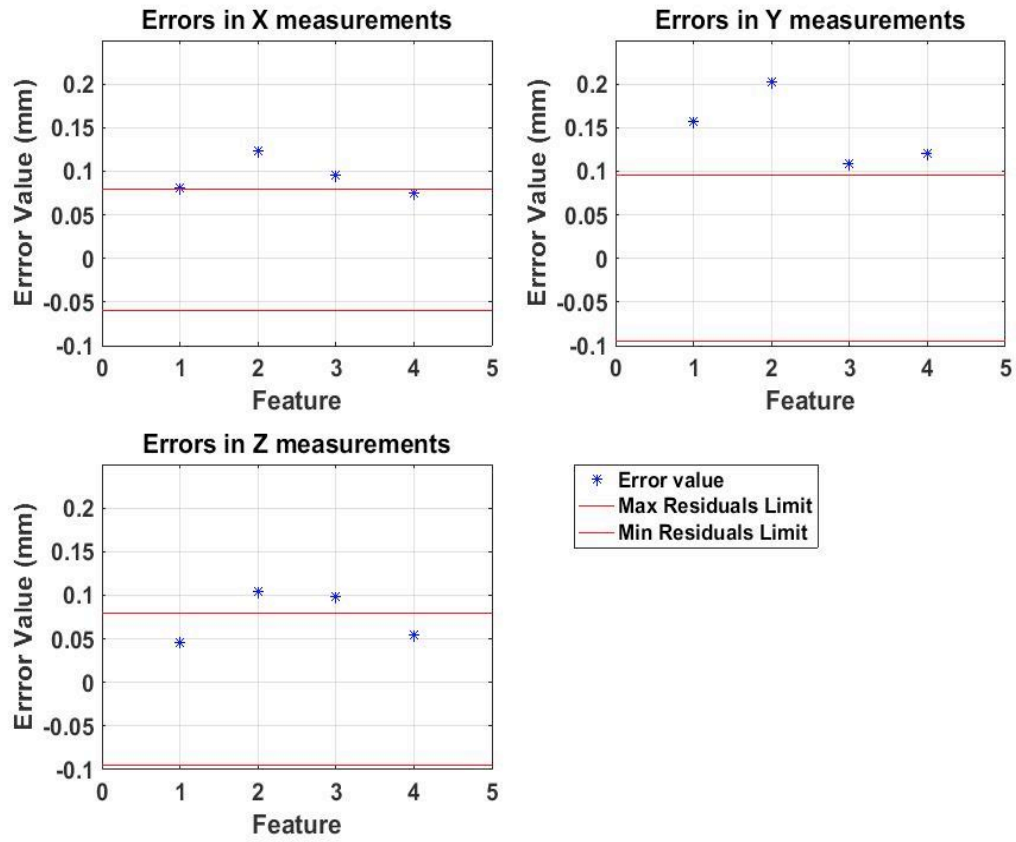
Figure 5.9: Error Evaluation for Part 5

6. DISCUSSION

6.1. ERROR VARIATION

If the effect of part location on one of the directional error say direction X is to be visualized on one can make use of the error model as given by equation 5. It is easy to plot different values of errors in X direction for a constant value of X location co-ordinate varying values of Y & Z location as illustrated in Figure 6.1
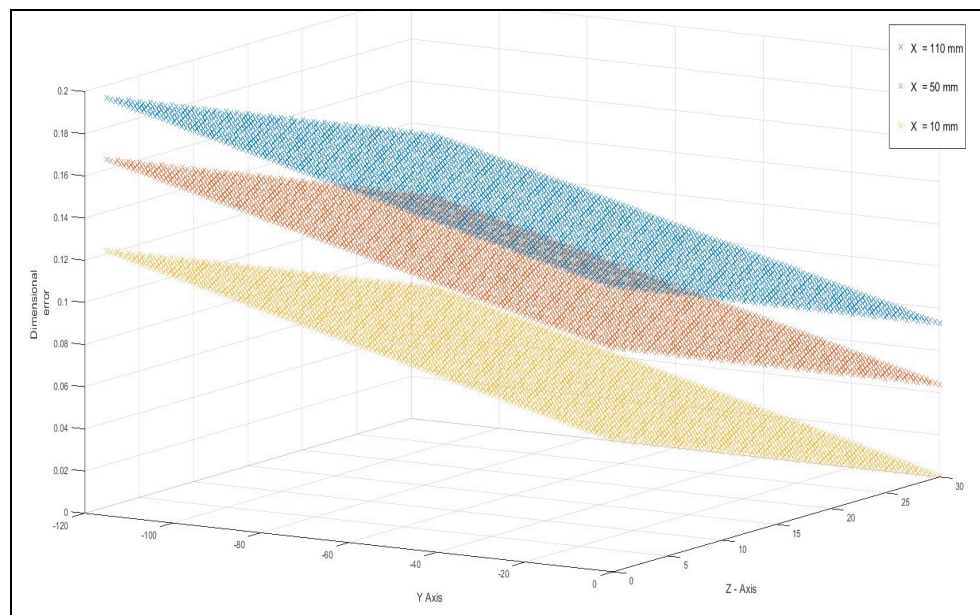
Figure 6.1: Variation of errors in X direction at constant X co-ordinate

From the Figure 6.1 it can be inferred that the error in X direction keeps on increasing from the origin towards the extremities of build chamber. Similar plots can be created for the errors in other two directions. Such trend in variation in error can be attributed to conditions, which alter from the center of the build plate towards the extremities of the build chamber. As mentioned in Section 3.2 all the processes

parameters are maintained at the same level for all four builds. Hence, it is safe to assume that the error variation is not caused by process parameters. However taking a closer look at laser scanning mechanism used by SLM machines one can argue that there the laser spot diameter may not remain the same throughout the build chamber. This is because in SLM machines a laser is placed stationary and the beam is rotated using a pair of galvo mirrors. The beam after reflecting form mirrors travels through a plano-convex lens. The lens aids in achieving a required spot diameter at specified distance. As the beam is supposed to originate in the center of the build chamber and scan a horizontal path within the chamber, it is intuitive to argue that laser spot would seem to be distorted throughout the build chamber. This argument can be better understood by referring to Figure 6.2. As can be seen from the Figure the beam is more distorted when it is scanning to laser path at point to the right rather than point on the left. Hence, at point on the right laser beam spot would be a elliptical in shape while laser beam spot at point on the left would be circular in shape.
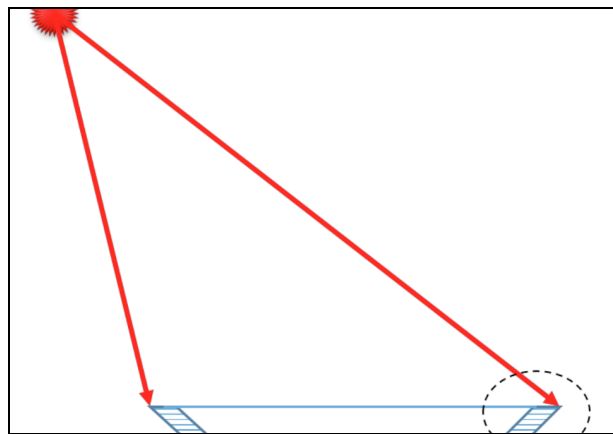
Figure 6.2: Laser spot deviation

However, most of the commercial SLM machines use F-Theta mechanism to specifically to address the issue of beam spot distortion. Using F-theta optics it is possible to achieve same spot size at different locations on the focal plane. In the current production set up i.e. Ranishaw AM250, similar F-theta optics principle is used for avoiding beam spot distortion (Mcmurtry, et al. 2015). Hence, it is not prudent to argue that variation in beam spot diameter could possibly be one of the important factors responsible for error variations within the build chamber. Some small in accuracies in the F-theta lens mechanism can lead to variation in spot diameter.

Even with the F-theta mechanism in place, the angle of incidence of scanning laser beam is different at different locations. The angle of scanning laser beam plays an important role in incident laser power. Also the laser beam has to travel through different locations throughout the build envelope. This means that the beam has to travel through different conditions of inert gas shielding, as the composition of gas is not maintained uniform throughout the chamber (Dadbakhsh S, 2012). Such different conditions for propagation of laser beam can lead to changes in laser power. In addition the irregularities in the compactness of the powder bed also plays an important role in surface inaccuracies. This phenomenon can be considered as an important cause for error variation in Z direction. The surface of powder bed is likely to have irregular flatness as the powder compacting is done based on flat surface at the bottom end of the powder bed. As the build platform moves down with each layer distance between top of the powder bed and the solid base keeps on changing. Thus surface irregularities are often seen on the surface of powder bed where the part has been build (Kleszczynski, Stefan, et al., 2012). Such inconsistencies may lead to multiple laser beam reflection there by altering

the beam power there by leading to dimensional inaccuracies (Meiners, Wilhelm, 1999). In this way a combination of multiple events such as inaccuracies in F-theta optics, different incidence angles of laser beam, beam scattering and diffusion due to different gas flow conditions within the build chamber, surface defects in the powder bed leads to variation of processing conditions within the build chamber. Hence a notable error variation can be observed through out the build chamber.

6.2.   PROBABLE APPLICATIONS OF THE ERROR MODEL

From the case study as discussed in Section 5 it is established that the error model can prove to be a useful tool for compensating errors for same geometry at different locations within the build chamber. Hence, these models can be useful in production of smaller batches of same geometry parts. These applications include functional components for aerospace industries, automotive racing industry, industrial applications such as pattern making, etc. The procedure can be tailored to include required build volume and with a fewer builds entire build layout can be modified to have minimum errors.

Other application of this approach can be cases where tight tolerance on of machining allowance is to be maintained. Having a capability of predicting the resulting dimensions for a giving part can not only lead to optimization of machining allowance but also checking for non-negative machining allowance for a given part. The non-negative machining allowance is a key requirement for parts where in post-processing applications such as polishing are required.

One of the findings of this research work is that the errors are distributed symmetrically along the centroid of the feature. Using such a feature based approach datum surface location problems can be addressed (Ameta, Gaurav, et al 2015).

7. CONLUSION AND FUTURE WORK

7.1. CONCLUDING COMMENTS

Using an exhaustive experimental analysis the variation of dimensional errors in each principle direction has been investigated in this research wok. With the multiple linear regression model fitting a tool for error compensation based on part location has been created. In addition, in process factors responsible for variation in dimensional errors across the build chamber are identified. The case study shown that the error compensation model can effectively offset the original dimension to meet the design specification saving cost and time for post processing operations. It was also concluded that the error model could not predict the dimensional error part having different geometry than the part used in calibration process. Hence, it was established that the difference in geometry has a significant effect on the part error.

7.2. FUTURE WORK

Following are the avenues, which could be further explored building on the foundation laid by current research work.

- It would be interesting to include the interaction terms within the error model fitted. Applicability of current error model can be compared with the error model including interaction.
- Study the effect of multiple linear regression model fitting to the data obtained by lesser number of experimental trials. In the other words, testing the effectiveness of an error model constructed using say a single build instead of four builds.

- Expansion of build volume to include entire build envelope with lesser number of parts or parts with scaled down volume in order to save the production time and cost.

- Conducting microstructural analysis of parts build at different locations can prove to be a useful data point in order to estimate position dependency of microstructure development.

APPENDIX A

LAY OUT DRAWING OF CALIBRATION PART
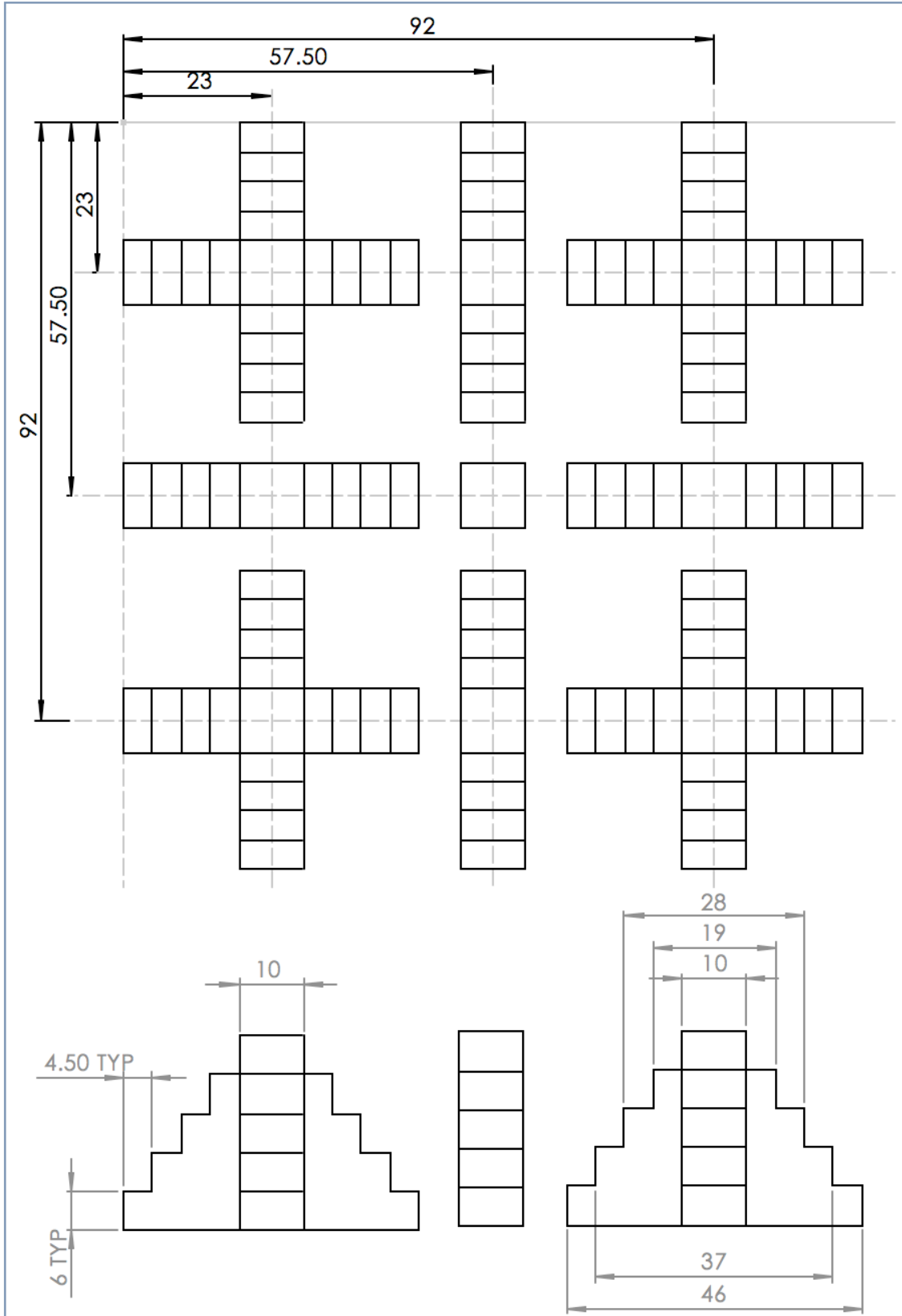
APPENDIX B

MATALB CODE FOR POINT CLOUD ALIGNMENT, PLANE FITTING AND
ERROR CALCULATION

```
clc;clear all; close all;
Px =
importdata('\\minerfiles.mst.edu\dfs\Users\nmkwdf\Desktop\Results\Corre
cted_data\Px_4.txt');
Py =
importdata('\\minerfiles.mst.edu\dfs\Users\nmkwdf\Desktop\Results\Corre
cted_data\Py_4.txt');
Pz =
importdata('\\minerfiles.mst.edu\dfs\Users\nmkwdf\Desktop\Results\Corre
cted_data\Pz_4.txt');
Zref
=importdata('\\minerfiles.mst.edu\dfs\Users\nmkwdf\Desktop\Results\Corr
ected_data\Z_Ref_4.txt');
Pal = [Px ;Py ;Pz ;Zref];
%% Making separate X planes
j=1;temp= zeros(40,1); % calculating x values
for i = 2:length(Px)
    temp(j,1)=ceil(Px(i-1,1));
    if (abs(Px(i,1)-Px(i-1,1))>2)
        j=j+1;
    end
end
j=1;
temp=sort(temp);
x_val= zeros(25,1);
for i = 2:length(temp)
    x_val(j)=temp(i-1);
    if (abs(temp(i)-temp(i-1))>2)
        j=j+1;
    end
end
x_val( ~any(x_val,2), : ) = [];

Sx_edge = zeros(156,3,20); % Planes including each step
siz = zeros (20,1);
for i = 1:length(Px);
    temp=[];
    for j=1 :length(x_val)
        if (abs(Px(i,1)-x_val(j,1))<2.5)
            temp = Sx_edge(:,:,j);
            temp( ~any(temp,2), : ) = [];
            Sx_edge(size(temp,1)+1,:,j)=Px(i,:);
            siz(j) = size(temp,1);
        end
    end
end
Sx_step = zeros(60,3,60);
for i = 1:20
    t = [1 1 1];
    temp = [];
    temp = Sx_edge(:,:,i);
    temp( ~any(temp,2), : ) = [];
    for j = 1:length(temp)
        if (temp(j,2)>-290)
            Sx_step(t(1),:,(i-1)*3 +1)=temp(j,:);
            t(1)= t(1)+1;
        elseif (temp(j,2)<-320)
```

```
                Sx_step(t(2),:,(i-1)*3 +2)=temp(j,:);
                t(2)= t(2)+1;
            else
                Sx_step(t(3),:,(i-1)*3 +3)=temp(j,:);
                t(3)= t(3)+1;
            end
        end
end


%% Making separate Y planes
plot3 (Py(:,1),Py(:,2),Py(:,3),'.');

j=1;temp= zeros(40,1); % calculating x values
for i = 2:length(Py)
    temp(j,1)=ceil(Py(i-1,2));
    if (abs(Py(i,2)-Py(i-1,2))>2)
        j=j+1;
    end
end
j=1; temp=sort(temp);
y_val= zeros(25,1);
for i = 2:length(temp)
    y_val(j)=temp(i-1);
    if (abs(temp(i)-temp(i-1))>2)
        j=j+1;
    end
end
y_val( ~any(y_val,2), : ) = [];


Sy_edge = zeros(156,3,20); % Planes including each step
for i = 1:length(Py);
    temp=[];
    for j=1 :length(y_val)
        if (abs(Py(i,2)-y_val(21-j,1))<2.5)
            temp = Sy_edge(:,:,j);
            temp( ~any(temp,2), : ) = [];
            Sy_edge(size(temp,1)+1,:,j)=Py(i,:);
            siz(j) = size(temp,1);
        end
    end
end


Sy_step = zeros(60,3,60);
for i = 1:20
    t = [1 1 1];
    temp = [];
    temp = Sy_edge(:,:,i);
    temp( ~any(temp,2), : ) = [];
    for j = 1:length(temp)
        if (temp(j,1)<190)
            Sy_step(t(1),:,(i-1)*3 +1)=temp(j,:);
            t(1)= t(1)+1;
        elseif (temp(j,1)>230)
            Sy_step(t(2),:,(i-1)*3 +2)=temp(j,:);
            t(2)= t(2)+1;
        else
```

```
                Sy_step(t(3),:,(i-1)*3 +3)=temp(j,:);
                t(3)= t(3)+1;
            end
        end
end
%% Making separate Z planes
p=Pz;
j=1;k=1;
for i = 1:length(p)
    if (p(i,1)<172)
        x(j,:)=p(i,:);
        j = j+1;
    elseif(p(i,1)> 182 && p(i,1)<203)
        x(j,:)=p(i,:);
        j = j+1;
    elseif(p(i,1)> 221 && p(i,1)<240.8)
        x(j,:)=p(i,:);
        j = j+1;
    elseif(p(i,1)> 251)
        x(j,:)=p(i,:);
        j = j+1;
    else
        y(k,:)=p(i,:);
        k= k+1;
    end
end


zx_val = [-365;-358;-352;-346];
zt= zeros(400,3,4);
for j=1:length(zx_val)
    k=1;
for i= 2:length(y)
    if(y(i,3)<zx_val(j))
        zt(k,:,j)=y(i,:);
        k=k+1;
        y(i,:)=[0 0 0];
    end
end
y( ~any(y,2), : ) = [];
end

% sorting along y direction
ylim = [-270;-300;-340;-370];
zx_edge = zeros(108,3,16);
for i =1:4
    temp = zt(:,:,i);
    temp( ~any(temp,2), : ) = [];
    for j=1:length(ylim)
        m=1;
        for k=1:length(temp)
        if(temp(k,2)>ylim(j))
            zx_edge(m,:,(i-1)*length(ylim)+j)=temp(k,:);
            m=m+1;
            temp(k,:)=-[1000 1000 1000];
        end
        end
```

```
    end
    temp=[];
end

% sorting along x direction
xlim= [190;230;255];
zx_step = zeros(50,3,48);
for i = 1:16
    temp= zx_edge(:,:,i);
    temp( ~any(temp,2), : ) = [];
    for j=1:length(xlim)
        m=1;
        for k=1:length(temp)
            if(temp(k,1)<xlim(j))
            zx_step(m,:,(i-1)*length(xlim)+j)=temp(k,:);
            m=m+1;
            temp(k,:)= [1000 1000 1000];
            end
        end
    end

end
zt= zeros(400,3,4);

for j=1:length(zx_val)
    k=1;
for i= 2:length(x)
    if(x(i,3)<zx_val(j))
        zt(k,:,j)=x(i,:);
        k=k+1;
        x(i,:)=[0 0 0];
    end
end
x( ~any(x,2), : ) = [];
end

% sorting along y direction
xlim= [175;220;245;280];
zy_edge = zeros(108,3,16);
for i =1:4
    temp = zt(:,:,i);
    temp( ~any(temp,2), : ) = [];
    for j=1:length(xlim)
        m=1;
        for k=1:length(temp)
        if(temp(k,1)<xlim(j))
            zy_edge(m,:,(i-1)*length(xlim)+j)=temp(k,:);
            m=m+1;
            temp(k,:)=+[1000 1000 1000];
        end
        end
    end
    temp=[];
end

% sorting along y direction
```

```
ylim= -[274;310;343];
zy_step = zeros(40,3,48);
for i = 1:16
    temp= zy_edge(:,:,i);
    temp( ~any(temp,2), : ) = [];
    for j=1:length(ylim)
        m=1;
        for k=1:length(temp)
            if(temp(k,2)>ylim(j)&& temp(k,2)<ylim(j)+15 )
            zy_step(m,:,(i-1)*length(ylim)+j)=temp(k,:);
            m=m+1;
            temp(k,:)= [1000 1000 1000];
            end
        end
    end

end

%% Face Normals & Plane Fitting
eqx_i=zeros(60,4);
Nx_i= zeros(60,3);
temp=[];
for i=1:60
    temp= Sx_step(:,:,i);
    temp( ~any(temp,2), : ) = [];
    [n,~,v]=affine_fit(temp);
    d= dot(v',n);
    eqx_i(i,:) =[n;-d]';
    Nx_i(i,:)=n';
end
eqx_e=zeros(20,4);
Nx_e= zeros(20,3);
temp=[];
for i=1:20
    temp= Sx_edge(:,:,i);
    temp( ~any(temp,2), : ) = [];
    [n,~,v]=affine_fit(temp);
    d= dot(v',n);
    eqx_e(i,:) =[n;-d]';
    Nx_e(i,:)=n';
end

eqy_i=zeros(60,4);
Ny_i= zeros(60,3);
temp=[];
for i=1:60
    temp= Sy_step(:,:,i);
    temp( ~any(temp,2), : ) = [];
    [n,~,v]=affine_fit(temp);
    d= dot(v',n);
    eqy_i(i,:) =[n;-d]';
    Ny_i(i,:)=n';
end
eqy_e=zeros(20,4);
Ny_e= zeros(20,3);
temp=[];
```

```
for i=1:20
    temp= Sy_edge(:,:,i);
    temp( ~any(temp,2), : ) = [];
    [n,~,v]=affine_fit(temp);
    d= dot(v',n);
    eqy_e(i,:) =[n;-d]';
    Ny_e(i,:)=n';
end

eqzx_i=zeros(48,4);
Nzx_i= zeros(48,3);
temp=[];
for i=1:48
    temp= zx_step(:,:,i);
    temp( ~any(temp,2), : ) = [];
    [n,~,v]=affine_fit(temp);
    d= dot(v',n);
    eqzx_i(i,:) =[n;-d]';
    Nzx_i(i,:)=n';
end
eqzx_e=zeros(16,4);
Nzx_e= zeros(16,3);
temp=[];
for i=1:16
    temp= zx_edge(:,:,i);
    temp( ~any(temp,2), : ) = [];
    [n,~,v]=affine_fit(temp);
    d= dot(v',n);
    eqzx_e(i,:) =[n;-d]';
    Nzx_e(i,:)=n';
end

eqzy_i=zeros(48,4);
Nzy_i= zeros(48,3);
temp=[];
for i=1:48
    temp= zx_step(:,:,i);
    temp( ~any(temp,2), : ) = [];
    [n,~,v]=affine_fit(temp);
    d= dot(v',n);
    eqzy_i(i,:) =[n;-d]';
    Nzy_i(i,:)=n';
end
eqzy_e=zeros(16,4);
Nzy_e= zeros(16,3);
temp=[];
for i=1:16
    temp= zx_edge(:,:,i);
    temp( ~any(temp,2), : ) = [];
    [n,~,v]=affine_fit(temp);
    d= dot(v',n);
    eqzy_e(i,:) =[n;-d]';
    Nzy_e(i,:)=n';
end
%% Alignment
```

```
[nz,~,vz] = affine_fit(Zref);
 z = vz(1,3);
C=[ -eqx_e(1,4)-eqx_e(1,3)*z ; -eqy_e(1,4)-eqy_e(1,3)*z ];
A=[ eqx_e(1,1) eqx_e(1,2); eqy_e(1,1) eqy_e(1,2)];
xy = ((A)^-1)*C;
pt = -[xy ;z];
M = makehgtform('translate',pt');
I = ones(length(Pal),1);
Pal1 = [Pal  I];
T1 = Pal1*M';

R = makehgtform('zrotate',0.5*0.0174533);
T = T1*R';

Ref1
=importdata('\\minerfiles.mst.edu\dfs\Users\nmkwdf\Desktop\Results\Corr
ected_data\Reference_Part.txt');



plot3 (T(:,1),T(:,2),T(:,3),'x',Ref(:,1),Ref(:,2),Ref(:,3),'.');
grid on; axis ([-inf,48,2,-48]);


%% dimensions calculation
temp=[];
u=1:3:58;

% X directions
distx= zeros(19,3);
for k =1:3
    datum = Sx_step(:,:,k);
    datum( ~any(datum,2), : ) = [];
    [nd,~,vd] = affine_fit(datum);
for i= 1:19
    distx(i,k) = abs([vd 1]*(eqx_i(u(i+1)+(k-1),:)')/norm(nd));
end
end

% Y directions
disty= zeros(19,3);
for k =1:3
    datum = Sy_step(:,:,k);
    datum( ~any(datum,2), : ) = [];
    [nd,~,vd] = affine_fit(datum);
for i= 1:19
    disty(i,k) = abs([vd 1]*(eqy_i(u(i+1)+(k-1),:)')/norm(nd));
end
end

% z_x direction
distzx= zeros(16,3);
datum = Zref;
datum( ~any(datum,2), : ) = [];
[n,~,v] = affine_fit(datum);
```

```
d = dot(v',n);
eq_i = [n ; -d];
t=1;
for i=1:16
    for j=1:3
    temp= zx_step(:,:,t);
    temp( ~any(temp,2), : ) = [];
    [nd,~,vd]=affine_fit(temp);
    distzx(i,j)= abs([vd 1]*eq_i/norm(nd))-0.09;
    t=t+1;
    end
end

% z_y direction
distzy= zeros(12,4);
datum = Zref;
datum( ~any(datum,2), : ) = [];
[n,~,v] = affine_fit(datum);
d = dot(v',n);
eq_i = [n ; -d];
t=1;
for i=1:12
    for j=1:4
    temp= zy_step(:,:,t);
    temp( ~any(temp,2), : ) = [];
    [nd,~,vd]=affine_fit(temp);
    distzy(i,j)= abs([vd 1]*eq_i/norm(nd))-0.1;
    t=t+1;
    end
end
```

APPENDIX C

MEASUREMENT DATA FOR CALIBRATION PART

Y Co-ordinate	Z Co-ordinate	Ref. Dim.	X =23			X =92		
			Measured Value	Error	% Error	Measured Value	Error	% Error
23	3	46	46.220	0.220	0.48	46.134	0.134	0.29
	9	37	37.188	0.188	0.51	37.136	0.136	0.37
	15	28	28.196	0.196	0.70	28.130	0.130	0.46
	21	19	19.182	0.182	0.96	19.137	0.137	0.72
	27	10	10.138	0.138	1.38	10.164	0.164	1.64
58	3	46	46.305	0.305	0.66	46.273	0.273	0.59
	9	37	37.285	0.285	0.77	37.242	0.242	0.65
	15	28	28.285	0.285	1.02	28.238	0.238	0.85
	21	19	19.247	0.247	1.30	19.199	0.199	1.05
	27	10	10.215	0.215	2.15	10.195	0.195	1.95
92	3	46	46.263	0.263	0.57	46.197	0.197	0.43
	9	37	37.234	0.234	0.63	37.176	0.176	0.48
	15	28	28.235	0.235	0.84	28.178	0.178	0.64
	21	19	19.215	0.215	1.13	19.169	0.169	0.89
	27	10	10.181	0.181	1.81	10.168	0.168	1.68

Y Co-ordinate	Z Co-ordinate	Ref. Dim.	X =23			X =92		
			Measured Value	Error	% Error	Measured Value	Error	% Error
23	3	46	46.2318	0.232	0.50	46.0645	0.064	0.14
	9	37	37.2333	0.233	0.63	37.1400	0.140	0.38
	15	28	28.1878	0.188	0.67	28.0996	0.100	0.36
	21	19	19.1694	0.169	0.89	19.1367	0.137	0.72
	27	10	10.1214	0.121	1.21	10.1415	0.142	1.42
58	3	46	46.2789	0.279	0.61	46.2213	0.221	0.48
	9	37	37.2969	0.297	0.80	37.2419	0.242	0.65
	15	28	28.2255	0.225	0.81	28.2005	0.200	0.72
	21	19	19.4431	0.443	2.33	19.2509	0.251	1.32
	27	10	10.1655	0.166	1.66	10.1575	0.158	1.58
92	3	46	46.2569	0.257	0.56	46.1803	0.180	0.39
	9	37	37.2560	0.256	0.69	37.2197	0.220	0.59
	15	28	28.2102	0.210	0.75	28.1677	0.168	0.60
	21	19	19.1873	0.187	0.99	19.1531	0.153	0.81
	27	10	10.1747	0.175	1.75	10.1626	0.163	1.63

Y Co-ordinate	Z Co-ordinate	Ref. Dim.	X =23			X =92		
			Measured Value	Error	% Error	Measured Value	Error	% Error
23	3	46	46.2198	0.220	0.48	46.1336	0.134	0.29

X Co-ordinate	Z Co-ordinate	Ref. Dim.	Y =23			Y =92		
			Measured Value	Error	% Error	Measured Value	Error	% Error
	9	37	37.1880	0.188	0.51	37.1361	0.136	0.37
	15	28	28.1959	0.196	0.70	28.1297	0.130	0.46
	21	19	19.1820	0.182	0.96	19.1371	0.137	0.72
	27	10	10.1379	0.138	1.38	10.1642	0.164	1.64
58	3	46	46.3049	0.305	0.66	46.2735	0.273	0.59
	9	37	37.2854	0.285	0.77	37.2420	0.242	0.65
	15	28	28.2853	0.285	1.02	28.2380	0.238	0.85
	21	19	19.2467	0.247	1.30	19.1989	0.199	1.05
	27	10	10.2149	0.215	2.15	10.1952	0.195	1.95
92	3	46	46.2634	0.263	0.57	46.1972	0.197	0.43
	9	37	37.2335	0.234	0.63	37.1764	0.176	0.48
	15	28	28.2348	0.235	0.84	28.1784	0.178	0.64
	21	19	19.2154	0.215	1.13	19.1692	0.169	0.89
	27	10	10.1806	0.181	1.81	10.1682	0.168	1.68
X Co-ordinate	Z Co-ordinate	Ref. Dim.	Y =23			Y =92		
			Measured Value	Error	% Error	Measured Value	Error	% Error
23	3	46	46.2603	0.260	0.57	46.4273	0.427	0.93
	9	37	37.1920	0.192	0.52	37.3116	0.312	0.84
	15	28	28.1614	0.161	0.58	28.3486	0.349	1.24
	21	19	19.1531	0.153	0.81	19.3180	0.318	1.67
	27	10	10.0985	0.098	0.98	10.2871	0.287	2.87
58	3	46	46.3009	0.301	0.65	46.4350	0.435	0.95
	9	37	37.2213	0.221	0.60	37.3601	0.360	0.97
	15	28	28.1648	0.165	0.59	28.3706	0.371	1.32
	21	19	19.2033	0.203	1.07	19.4029	0.403	2.12
	27	10	10.2030	0.203	2.03	10.3871	0.387	3.87
92	3	46	46.2569	0.257	0.56	46.2734	0.273	0.59
	9	37	37.2157	0.216	0.58	37.3778	0.378	1.02
	15	28	28.2056	0.206	0.73	28.2839	0.284	1.01
	21	19	19.1807	0.181	0.95	19.3455	0.345	1.82
	27	10	10.1984	0.198	1.98	10.2999	0.300	3.00
X Co-ordinate	Z Co-ordinate	Ref. Dim.	Y =23			Y =92		
			Measured Value	Error	% Error	Measured Value	Error	% Error
23	3	46	46.2023	0.202	0.44	46.2435	0.244	0.53
	9	37	37.2041	0.204	0.55	37.3313	0.331	0.90
	15	28	28.1575	0.158	0.56	28.3242	0.324	1.16
	21	19	19.1345	0.135	0.71	19.2810	0.281	1.48
	27	10	10.0701	0.070	0.70	10.2801	0.280	2.80
58	3	46	46.2603	0.260	0.57	46.4176	0.418	0.91
	9	37	37.2425	0.242	0.66	37.3910	0.391	1.06

| X Co-ordinate	Z Co-ordinate	Ref. Dim.	Y =23			Y =92		
			Measured Value	Error	% Error	Measured Value	Error	% Error
	15	28	28.2030	0.203	0.72	28.3584	0.358	1.28
	21	19	19.2015	0.201	1.06	19.3702	0.370	1.95
	27	10	10.1453	0.145	1.45	10.2904	0.290	2.90
92	3	46	46.2319	0.232	0.50	46.3284	0.328	0.71
	9	37	37.2153	0.215	0.58	37.3717	0.372	1.00
	15	28	28.1935	0.194	0.69	28.3374	0.337	1.21
	21	19	19.1726	0.173	0.91	19.3171	0.317	1.67
	27	10	10.1757	0.176	1.76	10.3150	0.315	3.15
X Co-ordinate	Z Co-ordinate	Ref. Dim.	Y =23			Y =92		
			Measured Value	Error	% Error	Measured Value	Error	% Error
23	3	46	46.1897	0.190	0.41	46.2294	0.229	0.50
	9	37	37.1715	0.171	0.46	37.2573	0.257	0.70
	15	28	28.1018	0.102	0.36	28.2504	0.250	0.89
	21	19	19.1572	0.157	0.83	19.2399	0.240	1.26
	27	10	10.0794	0.079	0.79	10.2135	0.214	2.14
58	3	46	46.2682	0.268	0.58	46.1587	0.159	0.34
	9	37	37.2113	0.211	0.57	37.2957	0.296	0.80
	15	28	28.2246	0.225	0.80	28.2859	0.286	1.02
	21	19	19.1810	0.181	0.95	19.2570	0.257	1.35
	27	10	10.1841	0.184	1.84	10.2396	0.240	2.40
92	3	46	46.2391	0.239	0.52	46.1481	0.148	0.32
	9	37	37.1986	0.199	0.54	37.2739	0.274	0.74
	15	28	28.2033	0.203	0.73	28.2541	0.254	0.91
	21	19	19.1893	0.189	1.00	19.2713	0.271	1.43
	27	10	10.1792	0.179	1.79	10.2381	0.238	2.38

APPENDIX D

SAS SAMPLE CODE AND RESIDUAL PLOTS FOR MODEL FITIING

SAS SAMPLE CODE

```
proc glm;
  class Xx Yx Zx;
  title3 'Interactive Model';
  model Xerror = Xx|Yx|Zx ;
  run;
```

RESIDUAL PLOTS

Residual Plots for X_error

Residual Plots for Y_error

Residual Plots for Z_error
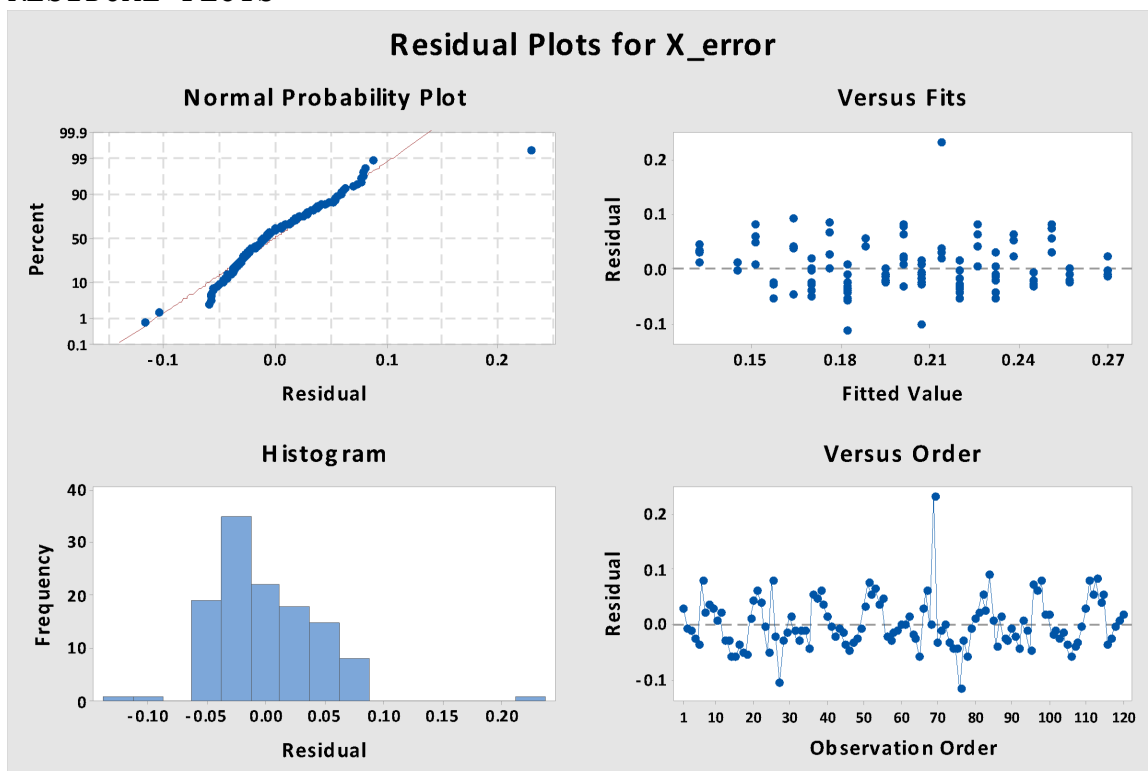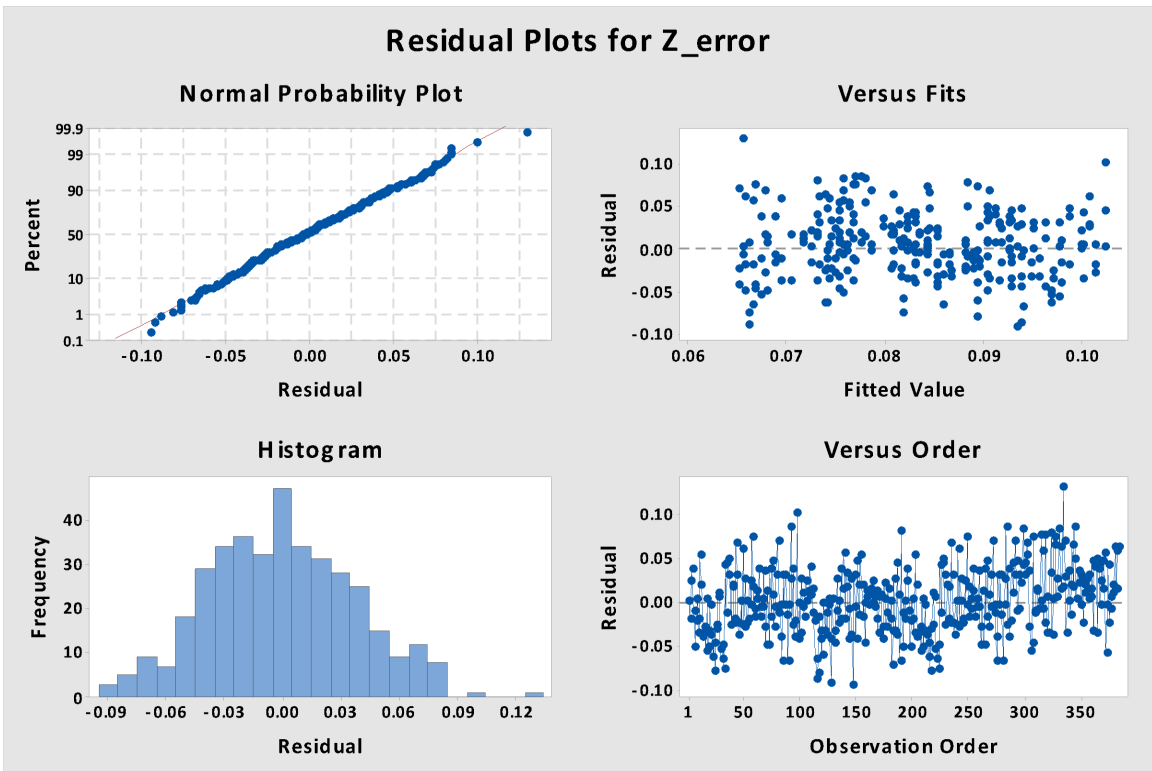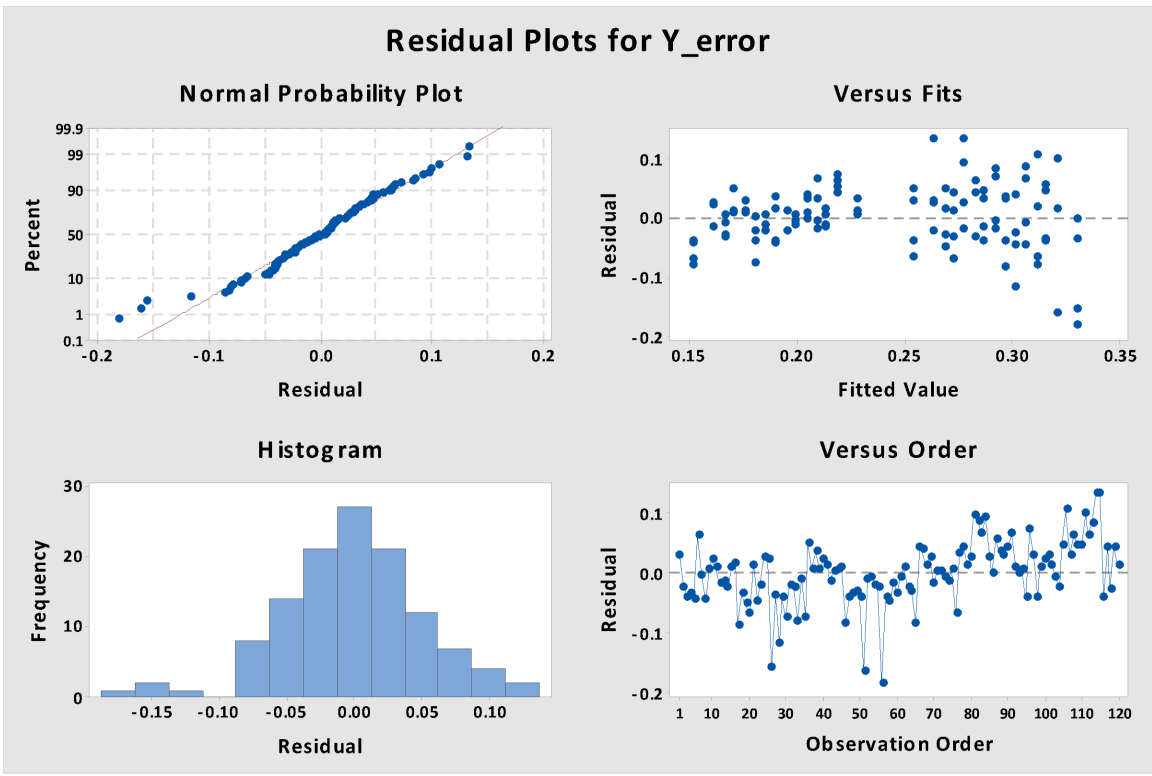
APPENDIX E

MEAUSERMENT VALUES FOR CASE STUDY

MEASUREMENT DATA FOR PART 1 & 3

Dimension	Specification Value (mm)	Part 1				Part 3		
		Compensation value(mm)	Measured value (mm)	Measured Error (%)	Error from Calibration Build#3 (%)	Compensation value(mm)	Measured value (mm)	Measured error (mm)
X1	46	45.854	46.078	0.17	0.48	45.835	46.022	0.022
X2	37	36.874	37.060	0.16	0.51	36.859	37.069	0.069
X3	28	27.847	28.077	0.28	0.70	27.835	28.011	0.011
X4	19	18.812	19.044	0.23	0.96	18.899	19.056	0.056
X5	10	9.851	10.101	1.01	1.38	9.847	10.065	0.065
Y1	46	45.973	46.097	0.21	0.41	45.688	46.071	0.071
Y2	37	36.854	37.096	0.26	0.46	36.797	37.021	0.021
Y3	28	27.790	28.047	0.17	0.36	27.770	28.065	0.065
Y4	19	18.790	19.109	0.57	0.83	18.668	19.028	0.028
Y5	10	9.854	10.099	0.99	0.79	9.790	10.079	0.079
ZX1	6	5.9437523	6.023	0.38	0.89	5.9437523	6.039	0.039
ZX2	12	11.9626783	12.076	0.63	1.00	11.9626783	12.005	0.005
ZX3	18	17.95677799	18.073	0.41	0.60	17.95677799	18.058	0.058

MEASUREMENT DATA FOR PART 2

Dimension	Specification Value (mm)	Part 2		
		Compensation value(mm)	Measured value (mm)	Measured error (mm)
X1	46	45.856	46.068	0.068
X2	37	36.775	37.053	0.053
X3	28	27.748	28.008	0.008
X4	19	18.773	19.066	0.066
X5	10	9.851	10.105	0.105
Z1	6	5.944	6.055	0.055
Z2	12	11.963	12.020	0.020
Z3	18	17.957	18.024	0.024
Z4	24	23.926	24.070	0.070
Z5	6	5.944	6.061	0.061
Z6	12	11.963	12.020	0.020
Z7	18	17.958	18.046	0.046
Z8	24	23.927	24.081	0.081

MEASUREMENT DATA FOR PART 4 AND 5

Dimension	Specification Value (mm)	Part 4			Part 5	
		Measured value (mm)	Measured Error (%)	Simulated error (%)	Measured value (mm)	Measured Error (mm)
X1	8	8.079	0.99	0.27	8.081	0.08
X2	8	8.101	1.26	0.34	8.123	0.12
X3	4	4.026	0.65	1.52	4.095	0.09
X4	8	8.065	0.81	1.36	8.075	0.07
Y1	40	40.256	0.64	1.57	40.157	0.16
Y2	30	30.203	0.68	1.56	30.202	0.20
Y3	6	6.058	0.97	0.55	6.108	0.11
Y4	6	6.061	1.02	0.32	6.12	0.12
Z1	4	4.042	1.05	1.76	4.045	0.04
Z2	14	14.111	0.79	2.16	14.105	0.11
Z3	14	14.105	0.75	2.10	14.099	0.10
Z4	6	6.053	0.88	1.50	6.054	0.05

BIBLIOGRAPHY

Ameta, Gaurav, et al. "Investigating the role of geometric dimensioning and tolerancing in additive manufacturing." Journal of Mechanical Design137.11 (2015): 111401.

Brøtan, Vegard. "A new method for determining and improving the accuracy of a powder bed additive manufacturing machine." The International Journal of Advanced Manufacturing Technology74.9-12 (2014): 1187-1195.

Castillo, Laura. "Study about the rapid manufacturing of complex parts of stainless steel and titanium." TNO report with the collaboration of AIMME(2005).

Dadbakhsh, S., L. Hao, and N. Sewell. "Effect of selective laser melting layout on the quality of stainless steel parts." Rapid Prototyping Journal 18.3 (2012): 241-249.

Eberly, David. "Least squares fitting of data." Chapel Hill, NC: Magic Software (2000).

Ferrar, B., et al. "Gas flow effects on selective laser melting (SLM) manufacturing performance." Journal of Materials Processing Technology212.2 (2012): 355-364.

Flack, David. "Measurement good practice Guide No. 42: CMM verification." National Physical Laboratory (2001).

Gockel, Joy, and Jack Beuth. "Understanding Ti-6Al-4V microstructure control in additive manufacturing via process maps." Solid Freeform Fabrication Proceedings, Austin, TX, Aug (2013): 12-14.

Huang, Qiang, et al. "Optimal offline compensation of shape shrinkage for three-dimensional printing processes." IIE Transactions 47.5 (2015): 431-441.

Iuliano, Luca, R. Ippolito, and A. De Filippi. "A new user part for performances evaluation of rapid prototyping systems." (1994): 327-339.

Kleszczynski, S., et al. "Position Dependency of Surface Roughness in Parts from Laser Beam Melting Systems." Proceedings of the 26th Internation Solid Freeform Fabrication (SFF) Symposium. 2015.

Kleszczynski, Stefan, et al. "Error detection in laser beam melting systems by high resolution imaging." Proceedings of the Solid Freeform Fabrication Symposium. 2012.

Klingbeil, N. W., et al. "Residual stress-induced warping in direct metal solid freeform fabrication." International Journal of Mechanical Sciences 44.1 (2002): 57-77.

Kruth, Jean-Pierre, et al. "Benchmarking of different SLS/SLM processes as rapid manufacturing techniques." (2005).

Li, Xudong, et al. "Automatic evaluation of machining allowance of precision castings based on plane features from 3D point cloud." Computers in Industry 64.9 (2013): 1129-1137.

Mcmurtry, David Roberts, et al. "ADDITIVE MANUFACTURING APPARATUS AND METHOD." U.S. Patent No. 20,160,136,730. 19 May 2016.

Meiners, Wilhelm. Direktes selektives Laser-Sintern einkomponentiger metallischer Werkstoffe. Shaker, (1999).

Montgomery, Douglas C. Design and analysis of experiments. John Wiley & Sons, 2008.

Moylan, Shawn, et al. "Proposal for a standardized test artifact for additive manufacturing machines and processes." 23rd Annual International Solid Freeform Fabrication Symposium, Austin, TX. (2012).

Paul, R., and S. Anand. "Material Shrinkage Modeling and Form Error Prediction in Additive Manufacturing Processes." Proceedings of the 41st NAMRC (2013).

Roberts, Ibiye Aseibichin. "Investigation of residual stresses in the laser melting of metal powders in additive layer manufacturing." (2012).

Snyder, Jacob C., et al. "Build Direction Effects on Microchannel Tolerance and Surface Roughness." Journal of Mechanical Design 137.11 (2015): 111411.

Strano, Giovanni, et al. "Surface roughness analysis, modeling and prediction in selective laser melting." Journal of Materials Processing Technology 213.4 (2013): 589-597.

Wang, Rong-Ji, et al. "Influence of process parameters on part shrinkage in SLS." The International Journal of Advanced Manufacturing Technology 33.5-6 (2007): 498-504.

Weisstein, Eric W. "Plane-Plane Intersection." (2002).

Zaeh, M. F., G. Branner, and T. A. Krol. "A three dimensional FE-model for the investigation of transient physical effects in Selective Laser Melting." 4th International Conference on Advanced Research in Virtual and Rapid Prototyping. (2010).

Zeng, Kai, Deepankar Pal, and Brent Stucker. "A review of thermal analysis methods in l aser sintering and selective laser melting." Proceedings of Solid Freeform Fabrication Symposium Austin, TX. (2012

VITA

Ninad Kulkarni was born in Kalyan, MH, India. He received his Bachelor of engineering degree in Mechanical Engineering from Datta Meghe College of Engineering, Airoli, Navi Mumbai affiliated to University of Mumbai, Kalina, India. He started his graduate degree program at Missouri University of Science and technology in January 2015. Here he worked as a research assistant under the guidance of Dr. Frank Liou on the topic "Error mapping of build volume in selective laser melting". In May 2017 he was awarded Master of Science degree in Manufacturing Engineering from Missouri University of Science and Technology, Rolla, Missouri, USA.